Ore Geology Reviews xxx (2008) xxx–xxx

Contents lists available at ScienceDirect

Ore Geology Reviews

journal homepage: www.elsevier.com/locate/oregeorev

Gold-oxysulphides in copper deposits of the Greywacke Zone, Austria: A mineral chemical and infrared fluid inclusion study

Henryk Kucha [a], Johann G. Raith [b,*]

[a] University of Mining & Metallurgy, 30-059 Krakow, Mickiewicza 30, Poland
[b] Department of Applied Geosciences and Geophysics, University of Leoben, Peter Tunner-Straße 5, A-8700 Leoben, Austria

ARTICLE INFO

Article history:
Received 12 December 2007
Received in revised form 24 October 2008
Accepted 24 October 2008
Available online xxxx

Keywords:
Gold
Oxysulphides
Tetrahedrite
Fluid inclusions
Infrared microthermometry
Eastern Alps
Thiosulphate
Cu deposits

ABSTRACT

Native gold and unusual gold-oxysulphides, both associated with tetrahedrite, occur in several abandoned copper deposits in the low grade Palaeozoic Greywacke Zone in the Eastern Alps. The ore mineralogy, the mineral chemistry and fluid inclusions in tetrahedrite and quartz were studied from historic Cu mines at Larzenbach/Hüttau, St. Veit im Pongau, and Mitterberg (all Salzburg Province, Austria). Fluid inclusions in tetrahedrite, which is non-transparent in visible light, were studied by infrared (IR) microthermometry; tetrahedrite containing up ~2.5 wt.% As is transparent for infrared light.

Fluid inclusions within tetrahedrite occur as isolated inclusions, in clusters and along trails. At room temperatures these are aqueous two-phase liquid (L)+vapour (V) inclusions of low to moderate total salinity (T_m −3 to −14 °C). Homogenisation temperatures (T_h V→L) range between 85 and 200 °C. The composition of these tetrahedrite-hosted fluid inclusions corresponds to that one type of fluid inclusion in quartz showing a similar range in salinity (T_m −3 to −12 °C) and total homogenisation temperatures (T_h V→L, 71.5 to 250 °C). Another type of higher saline aqueous two-phase (L+V) inclusions in quartz is apparently unrelated to gold mineralisation.

Fluid inclusions within tetrahedrite coexist with small solid inclusions of chalcopyrite, gold-oxysulphides, minor arsenopyrite and gold that is rich in gold-oxysulphide microinclusions and occur along re-healed microfractures within tetrahedrite. These microfractures also control the replacement of As-poor tetrahedrite by arseniferous (up to 3.16 wt.% As) tetrahedrite. It is suggested that in addition to cooling the exchange of As for Sb on tetrahedrite surfaces was one of the factors controlling precipitation of gold. Oxysulphides are associated with (a) native gold in unweathered primary ores and (b) remobilised Cu-rich gold in weathered ores. Gold thiosulphate and possibly thioarsenite complexes are the preferred species for the transport of gold in the low-temperature (<250 °C) hydrothermal fluids and gold thiosulphate complexes were involved in the supergene remobilisation of gold.

1. Introduction

Oxoacids of sulphur such as thiosulphate, thionate or sulphite form as transitional species during the oxidation of reduced sulphur to sulphate, or vice versa, during reduction of sulphate to sulphide sulphur (e.g., Goldhaber, 1983; Greenwood and Earnshaw, 1984). Oxysulphides can be defined as solid chemical compounds incorporating sulphur as well as oxygen in their structure in addition to metallic cations (M). They are distinguished from sulphates by their different sulphur to oxygen ratio and especially by different mixed sulphur valence; e.g., thiosulphate, $M^{2+}S_2O_3$ with S:O of 2:3 and an average sulphur valence of $^{2+}$, where half of the sulphur is S^{2-} and the other half S^{6+}. Copper, Fe, Ni, Ba, Ca and Pb are some of the more common metals that combine with oxoacids of sulphur, though precious metals such as Au, Ag, PGE can also form solid mixed sulphur valence compounds such as gold–copper oxysulphides dealt with in this paper.

Only a few compounds with mixed or intermediate sulphur valences have so far been accepted by the International Mineralogical Association (IMA-CNMMN) as minerals. These include: scotlandite $PbSO_3$ (Paar et al., 1984), hannebachite $CaSO_3{\cdot}0.5H_2O$ (Hentschel et al., 1985), gravegliaite $MnSO_3{\cdot}3H_2O$ (Basso et al., 1991), bazhenovite $CaS_5{\cdot}CaS_2O_3{\cdot}6Ca(OH)_2{\cdot}20H_2O$ (Chesnokov et al., 1987), and viaenite $(Fe,Pb)_4S_8O$ (Kucha et al., 1996). From a mineralogical perspective, oxysulphides are therefore interesting as a rare group of possibly new minerals.

Mineralogically less well-characterised oxysulphides have been reported from several gold deposits before by the first author. None of these phases has so far been accepted as a new mineral, mostly because of lacking structural data; the phases are normally too small for structural analysis. The phases reported so far include iron thiosulphates associated with pyrite and gold from mesothermal vein-type gold deposits in eastern Australia and South Africa (Kucha

* Corresponding author. Tel.: +43 3842 402 6213; fax: +43 3842 47016.
E-mail address: johann.raith@unileoben.ac.at (J.G. Raith).

0169-1368/$ – see front matter © 2008 Elsevier B.V. All rights reserved.
doi:10.1016/j.oregeorev.2008.10.004

et al., 1994), the Amelia Mine, Southwest Wisconsin (Kucha and Barnes, 1995) as well as copper thiosulphates and gold oxysulphides associated with gold in Cu-ores in the Greywacke Zone of the Eastern Alps (Fig. 1; Kucha et al., 1995, 1997b, 2003). In this paper we provide further evidence that these easily overlooked phases are distributed on a regional to orogenic scale within the Eastern Alps and could be possibly neglected as carriers of gold.

From experimental studies it is known that thiosulphates are stable below ~240 °C (Giggenbach, 1974) in the near neutral to slightly alkaline pH range and under intermediate redox conditions (Webster, 1986). Hence, thiosulphate complexes of gold can be expected to occur in lower temperature hydrothermal to supergene ore deposits. They were for example confirmed in hydrothermal fluids in geothermal systems (e.g., hot springs in Waiotapu, New Zealand and Yellowstone, U.S.A.; Xu et al., 1998; Pope et al., 2005) and seem to be of special importance for the mobilisation of gold in the supergene environment (Webster, 1986; Benedetti and Boulegue, 1991; Bowell et al., 1993).

Finally, the presence of oxysulphides in gold ores has practical implications for the recovery of gold in hydrometallurgical processes. The capacity of thiosulphate complexes for low-temperature leaching of gold has been intensely studied by hydrometallurgists because thiosulphate leaching may be an environment-friendly alternative to cyanide leaching of gold ores (see review by Aylmore and Muir, 2001).

The aims of this paper are: (1) to document the occurrence and mineral chemical composition of native gold and associated tetrahedrite and gold oxysulphides in the Greywacke Zone, Eastern Alps; (2) to constrain the T–X conditions of fluids involved in formation of gold-bearing ore assemblages by using infrared (IR) microthemometry; (3) to discuss the relevance of our findings for understanding the transport and mobilisation of gold in low-temperature hydrothermal and supergene environments.

2. Geological setting

Geologically, the gold occurrences studied are located in the Greywacke Zone, which is part of the Upper Austroalpine very low- to low-grade basement units of the Eastern Alps (Ebner, 1997). It is subdivided into the Eastern (EGZ) and Western Greywacke Zone (WGZ, Fig. 1). The Eastern Greywacke Zone consists of metavolcano-sedimentary rocks of Palaeozoic age and is further subdivided into four Alpine-age tectonic nappes (Neubauer et al., 1994). The two most important of these are the tectonically deeper Veitsch nappe and the tectonically higher Noric nappe. The Veitsch nappe includes Early Carboniferous to Permian clastic and carbonate metasediments, the Noric nappe contains metamorphosed Ordovician to Namurian clastic to carbonate shelf and slope sediments, as well as felsic metavolcanics of Ordovician and metabasites of Silurian age.

Two major tectonic units are also distinguished in the Western Greywacke Zone. The northern Wildseeloder unit with Late Ordovician metaignimbrites and Silurian to Devonian carbonate platform sediments and the southern Glemmtal unit with a several thousand metres thick sequence of siliciclastic rocks deposited in a marine basin at a passive continental margin (Heinisch, 1988). The intra-plate geochemical characteristics of Late Devonian mafic volcanism is also consistent with this interpretation (Heinisch, 1988).

Regional metamorphism in the Eastern Greywacke Zone is of very low- to low-grade and is predominantly of Eoalpine (i.e., Cretaceous) age (Hoinkes et al., 1999). Metamorphic conditions transitional between sub-greenschist and greenschist facies are recorded from higher structural levels in the Western Greywacke Zone (e.g., around Mitterberg; Kralik et al., 1987) and generally increase to lower greenschist facies conditions towards the lower structural units. Metamorphic conditions of about 450 °C and 0.3 to

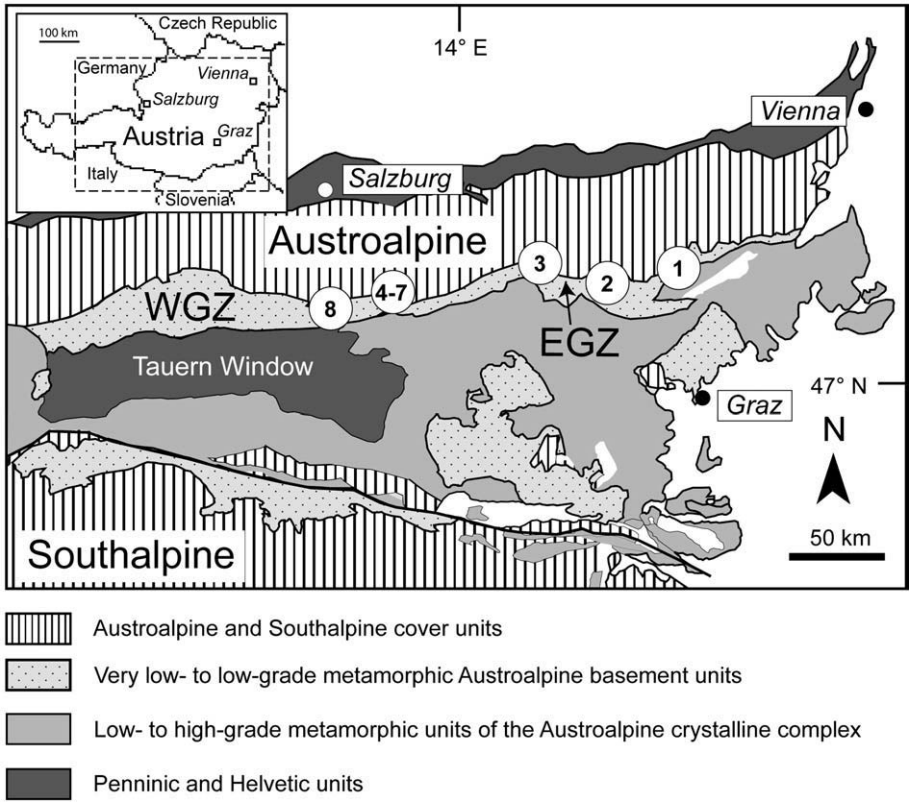

Fig. 1. Geological sketch map of part of the Eastern Alps showing locations of gold occurrences in the Greywacke Zone (EGZ Eastern Greywacke Zone, WGZ Western Greywacke Zone). 1 Veitsch, 2 Erzberg/Eisenerz siderite mine, 3 Rottenmann, 4–7 Larzenbach/Hüttau, Igelsbach, Giellach, St. Veit im Pongau, 8 Mühlbach am Hochkönig (Mitterberg Südrevier).

Please cite this article as: Kucha, H., Raith, J.G., Gold-oxysulphides in copper deposits of the Greywacke Zone, Austria: A mineral chemical and infrared fluid inclusion study, Ore Geology Reviews (2008), doi:10.1016/j.oregeorev.2008.10.004

Table 1
Chemical composition (wt.%) of tetrahedrite from Larzenbach (LA) and St Veit im Pongau (SV), Salzburg Province, Austria

	LA1 A9	LA1 A10	LA1 A11	LA1 A2	LA2 A9	LA2 A11	LA2 A20	LA2 A21	LA2 A23	LA2 A24	LA2 A25	LA2 A26	LA2 A27	LA2 A28	LA2 A29	LA2 A15	LA2 B2	LA2 C2	SV 1003A3	SV2 B1
Cu	41.76	40.96	40.48	39.68	40.93	38.98	41.76	40.41	40.88	37.47	39.37	39.71	39.86	38.89	39.73	38.20	39.33	39.69	37.89	37.34
Ag	0.05	0.05	0.05	0.40	≤0.04	0.92	≤0.04	0.09	≤0.04	0.84	0.14	0.05	≤0.04	≤0.04	0.33	0.23	0.18	0.93	0.73	0.13
Au	≤0.04	≤0.04	≤0.04	≤0.04	≤0.04	4.60	≤0.04	≤0.04	≤0.04	0.10	≤0.04	≤0.04	≤0.04	≤0.04	≤0.04	0.54	0.08	≤0.04	≤0.04	≤0.04
Fe	3.88	3.90	3.83	3.26	3.76	4.30	4.17	4.11	4.23	5.39	4.30	4.08	4.00	4.18	4.12	4.53	3.70	3.32	3.40	3.70
Zn	1.95	2.00	2.35	2.58	2.14	≤0.02	1.87	1.56	1.54	1.96	1.79	1.81	1.54	1.68	1.76	1.98	2.00	2.45	4.80	3.40
Hg	0.30	0.46	0.15	0.60	1.04	≤0.05	≤0.05	0.75	0.30	0.60	≤0.05	0.30	0.45	0.60	0.60	0.15	0.45	≤0.05	0.30	0.06
As	2.73	2.96	2.70	2.51	2.90	19.98	2.86	2.00	2.41	2.19	2.97	2.97	2.94	2.94	3.06	2.43	2.69	2.70	1.22	0.91
Sb	24.10	23.96	24.39	24.63	23.00	0.71	23.78	24.75	24.68	24.97	25.26	25.03	25.48	25.25	25.16	25.65	25.76	24.95	26.24	28.38
S	25.73	24.66	25.47	25.89	25.50	27.91	26.38	25.75	25.98	25.02	25.54	25.77	25.18	25.54	25.60	25.54	25.37	24.86	24.25	25.46
Total	100.50	98.95	99.42	99.55	99.27	97.70	100.82	99.42	100.02	98.54	99.37	99.57	99.45	99.08	100.36	99.25	99.56	98.90	98.83	99.32
Normalised to 13 S																				
Cu	10.646	10.897	10.424	10.055	10.530	9.163	10.386	10.296	10.323	9.825	10.113	10.109	10.385	9.990	10.182	9.813	9.890	10.186	10.251	9.622
Fe	1.126	1.180	1.122	0.940	1.101	1.230	1.180	1.191	1.215	1.608	1.257	1.182	1.186	1.222	1.201	1.324	1.089	0.997	1.047	1.085
Ag	0.008	0.008	0.008	0.060	–	0.127	–	0.014	–	0.130	0.021	0.008	–	–	0.050	0.035	0.027	0.145	0.116	0.020
Au	–	–	–	–	–	0.348	–	–	–	–	–	–	–	–	–	0.045	0.007	–	–	–
Zn	0.483	0.517	0.036	0.635	0.535		0.452	0.386	0.378	0.500	0.447	0.448	0.390	0.419	0.438	0.494	0.503	0.628	1.262	0.851
Hg	0.024	0.039	0.012	0.048	0.085	–	–	0.061	0.024	0.050	–	0.024	0.037	0.049	0.049	0.012	0.037	–	0.026	0.005
As	0.590	0.668	0.591	0.540	0.633	3.984	0.603	0.432	0.516	0.487	0.647	0.609	0.650	0.641	0.665	0.530	0.590	0.604	0.280	0.199
Sb	3.206	3.326	3.278	3.256	3.087	0.087	3.086	3.290	3.252	3.416	3.386	3.325	3.464	3.384	3.364	3.438	3.476	3.435	3.704	3.816
Sb/(Sb+As)	0.84	0.83	0.85	0.86	0.83	0.02	0.84	0.88	0.86	0.88	0.84	0.85	0.84	0.84	0.83	0.87	0.85	0.85	0.93	0.95

≤ — below indicated detection limit.

0.4 GPa have been suggested for the Veitsch nappe (Ratschbacher and Klima, 1985). The study of carbonaceous material much better quantified metamorphic temperatures during Eoalpine thrusting (Rantitsch et al., 2004); they were 360±30 °C and confirm metamorphic temperatures recorded from the Veitsch nappe (360 to 410 °C, >0.2 GPa at the Kaisersberg graphite mine; Raith and Vali, 1998).

3. Gold-bearing copper occurrences in the Greywacke Zone

Gold associated with tetrahedrite has been confirmed from the following locations (Fig. 1): Veitsch magnesite quarry, Erzberg siderite mine at Eisenerz, Rottenmann, and the abandoned historic copper deposits at Larzenbach, Giellach, Igelsbach, St. Veit im Pongau, Mühlbach am Hochkönig, and Mitterberg.

Table 2
Chemical composition (wt. %) of gold from Larzenbach (samples LA1 and LA2) and St. Veit im Pongau (sample SV1003 Mitterainberg; sample SV2 Teufelrauchfang), Salzburg Province, Austria

Sample/spot	Au	Ag	Cu	Hg	Fe	As	Sb	S	Ni	Sum	Host mineral
LA1 A1	68.03	21.21	3.88	7.17	≤0.02	≤0.05	0.33	≤0.04	na	100.62	Fracture in tetrahedrite
LA1 A5	54.74	25.59	3.04	15.66	0.42	0.17	0.80	0.16	na	100.58	Fracture in tetrahedrite
LA1 B1	56.75	20.36	1.05	21.25	≤0.02	≤0.05	0.17	≤0.04	na	99.58	Fracture in tetrahedrite
LA1 C1	64.64	22.08	3.90	7.44	0.62	≤0.05	1.00	0.55	na	100.23	Tetrahedrite
LA1 C2	68.84	14.87	9.98	2.28	1.63	≤0.05	2.13	0.55	na	100.28	Oxysulphide Type 2 in tetrahedrite
LA1 C3	65.68	4.70	22.07	2.27	1.87	≤0.05	1.04	1.06	na	98.69	Oxysulphide Type 2 in tetrahedrite
LA1 C4	76.45	7.23	9.58	2.55	1.79	≤0.05	2.31	0.81	na	100.72	Oxysulphide Type 2 in tetrahedrite
LA1 C5	80.61	6.21	8.67	1.20	1.86	≤0.05	1.91	0.80	na	101.26	Oxysulphide Type 2 in tetrahedrite
LA1 D3	78.31	14.26	0.77	5.05	0.37	≤0.05	≤0.04	≤0.04	na	98.76	Tetrahedrite surface
LA1 D4	63.82	1.67	2.73	1.64	1.98	3.81	1.78	1.25	na	78.68	Oxysulphide Type 1? in tetrahedrite
LA1 D5	62.36	1.78	3.96	1.26	1.60	4.87	1.66	2.00	na	79.49	Oxysulphide Type 2? in tetrahedrite
LA2 A1	75.09	13.65	2.15	6.57	0.17	0.08	0.20	≤0.04	na	97.91	Oxysulphide Type 1 in tetrahedrite
LA2 A5	75.84	16.97	2.63	4.66	0.47	≤0.05	0.20	≤0.04	na	100.77	Oxysulphide Type 1 in tetrahedrite
LA2 A6	75.75	14.59	2.52	4.17	0.25	≤0.05	0.37	≤0.04	na	97.65	Oxysulphide Type 1in tetrahedrite
LA2 A10	78.77	13.00	2.13	5.18	≤0.02	≤0.05	0.10	≤0.04	na	99.08	Oxysulphide Type 1 in tetrahedrite
LA2 B1	87.85	4.84	2.85	5.18	≤0.02	≤0.05	0.14	≤0.04	na	100.86	$CuFeS_2$
LA2 C1	79.70	15.46	1.87	4.58	≤0.02	≤0.05	0.07	≤0.04	na	101.68	Fracture in tetrahedrite
LA2 C2a	79.84	15.24	1.90	4.58	≤0.02	≤0.05	0.10	≤0.04	na	101.66	Fracture in tetrahedrite
LA2 D1	80.42	9.44	2.43	7.55	0.12	≤0.05	0.51	≤0.04	na	100.47	Fracture in tetrahedrite
LA2 D2	72.35	5.25	4.76	3.79	0.21	1.02	1.97	0.23	na	89.58	Oxysulphide 2? in tetrahedrite
LA2 D3	81.33	12.39	1.79	5.79	0.21	0.08	0.10	≤0.04	na	101.69	Fracture in tetrahedrite
LA2 D7	73.36	5.55	2.91	4.06	1.13	0.17	1.67	0.13	na	88.81	Oxysulphide Type 1?
LA2 E2	83.70	6.11	1.95	7.11	≤0.02	≤0.05	≤0.04	≤0.04	na	98.47	Fracture in calcite
SV1003 A1	70.62	≤0.06	21.22	≤0.06	0.21	0.64	4.83	2.71	na	100.23	Fe–Cu oxide
SV1003 C1	80.93	7.90	4.60	4.68	0.20	≤0.06	2.73	0.47	na	101.51	Cu–Fe oxide
SV1003 C2	82.89	≤0.06	7.92	4.31	0.08	≤0.06	3.29	0.11	na	98.64	Cu–Fe oxide
SV1003 B2	79.02	12.49	1.80	7.12	≤0.06	≤0.06	≤0.06	≤0.04	na	100.43	$CuFeS_2$
SV1003 B3	76.80	14.22	1.47	7.74	≤0.05	<0.06	≤0.06	≤0.04	na	100.23	$CuFeS_2$
SV1003 B4	75.46	1.18	8.27	≤0.06	0.09	0.96	11.91	1.01	na	98.88	Cu–Fe oxide
SV1003 B5	68.19	2.31	12.73	≤0.06	0.10	1.06	12.70	3.76	na	100.85	Cu–Fe oxide
SV1003 B6	69.38	1.51	10.06	≤0.06	0.08	0.61	15.73	2.26	na	99.63	Cu–Fe oxide
SV2 B3	96.79	3.02	0.34	≤0.06	≤0.05	1.37	0.24	0.11	≤0.05	101.87	FeAsS
SV2 B4	91.67	2.63	1.07	≤0.06	0.55	0.39	0.83	1.05	0.5	98.69	FeAsS
SV2 B5	89.35	2.34	0.42	≤0.06	0.61	4.15	0.29	1.22	0.33	98.71	FeAsS

na not analysed; ≤ below indicated detection limit.

Please cite this article as: Kucha, H., Raith, J.G., Gold-oxysulphides in copper deposits of the Greywacke Zone, Austria: A mineral chemical and infrared fluid inclusion study, Ore Geology Reviews (2008), doi:10.1016/j.oregeorev.2008.10.004

This study focuses on gold-bearing Cu mineralisation at Larzenbach/Hüttau and St. Veit im Pongau where small-scale historical mining took place between the 13th and 18th Centuries (Günther, 1978). These occurrences are part of the copper district Mitterberg–Mühlbach–Larzenbach where the largest Cu mine of the Eastern Alps located at Mitterberg (total Cu content ca. 250,000 t; Weber, 1997) was mined until the 1970s. Details about gold mineralisation and oxysulphides from Mitterberg and Veitsch have been published previously (Kucha et al., 1995, 1997a,b).

The ores at Larzenbach are hosted by low-grade metasedimentary rocks (phyllites, black schists, quartzites), metabasites and metatuffs and, at St. Veit, in metacarbonates (marbles, calcareous phyllites). Stratabound as well as clearly discordant vein-type ores are known. At Larzenbach the main orebody is lens-shaped and was mined ca. 170 m along strike and ca. 60 m along depth. The NW-striking orebody has a maximum thickness of 8 m and dips at ca. 40–50° to the NE. Whereas thin cm to dm-thick ore stringers are mostly concordant to the main foliation, the major vein locally exhibits clear discordant contacts between ore and the main foliation. At Larzenbach the ores were affected by several ductile and brittle deformation events causing an irregular distribution and discontinuity of the orebodies (Feitzinger, 2000). The average gold content in tetrahedrite-rich ore is 4 g/t (Günther, 1978).

Vein-type copper mineralisation at Mitterberg ("Hauptgang") is clearly discordant and connected to an 11 km long and 0.2 to 4 m thick carbonate-quartz vein of Cretaceous age (for references see Weber, 1997). In contrast, orebodies south of Mitterberg ("Mühlbach Südrevier") lie concordant within the host rocks (Weber et al., 1972). The main ore minerals in these Cu-dominated ores are chalcopyrite, tetrahedrite and minor Ni–Co minerals. Common gangue minerals are quartz and Fe-carbonates.

Gold contents of ~11 g/t in tetrahedrite were reported from Mitterberg by Böhme (1931). He described a paragenesis of native gold, tetrahedrite, gersdorffite and chalcopyrite from the younger sulphide-quartz veins that postdate the main Cu vein. Spectacular specimens of native gold associated with U–Ni–Te mineralisation were found in the uppermost part of the Mitterberg Cu vein where the vein crosscuts Carboniferous–Permian metaclastic host rocks (Paar and Köppel, 1978). Uraninite from this paragenesis was dated at 90±5 Ma (Köppel in Paar and Köppel, 1978). This age confirms that the main Cu vein at Mitterberg formed during the Eoalpine orogeny.

4. Methods

Samples were polished on a Rehwalt polishing machine using light oil as a lubricant. Final polishing was done with 1 µm diamond spray. Water has been avoided as a lubricant because it causes dissolution of oxysulphides present in these samples.

Microanalysis and fluid inclusion study were carried out at the fluid inclusion laboratory of the Department of Applied Geosciences and Geophysics, University of Leoben. The chemical compositions of mineral phases and valence-related SKα and SKβ peak shifts were determined with an ARL SEMQ automated electron microprobe (EMP). For principles and details regarding valence determination of sulphur by EMP the reader is referred to Kucha et al. (1989, 1995). Gold valences in oxysulphides were measured by EMP at 23 kV using the normalised Au Mβ/Mα emission efficiency ratios compared to standards of metallic gold (valence 0, Mβ/Mα = 0.8003 ± 0.0029), $AuTe_2$ (valence +1, Mβ/Mα = 0.8079 ± 0.0034), and $AuBr_3$ (valence +3, Mβ/Mα = 0.7655 ± 0.0230 (Kucha et al., 1998; Kucha and Przylowicz, 1999).

Infrared (IR) microthermometric measurements on tetrahedrite were accomplished in transmitted light using an Infrared CCD camera (λ ≤ 2.5 µm) attached to an Olympus BX60 microscope. Cooling–heating experiments were performed with a Linkam MDS 600 stage. Synthetic fluid inclusions were used for calibration. The accuracy of the measurements were ±1 °C during heating and ±0.5 °C during freezing runs. Total salinities of salt-bearing aqueous fluid inclusions and bulk densities were calculated from the final ice melting temperatures (T_m) and the total homogenisation temperatures (T_h) using the software package FLUIDS 1 by Bakker (2003). Total salinities are given as mass % NaCl equivalent or mass % $CaCl_2$ equivalent (when T_m was below the eutectic temperature of the pure H_2O–NaCl system).

5. Ore mineralogy, mineral chemistry and valence determinations

5.1. Tetrahedrite–tennantite series

Members of the tetrahedrite–tennantite series are mostly Sb-dominated (Table 1) and classified as tetrahedrite. The ratio Sb/As in

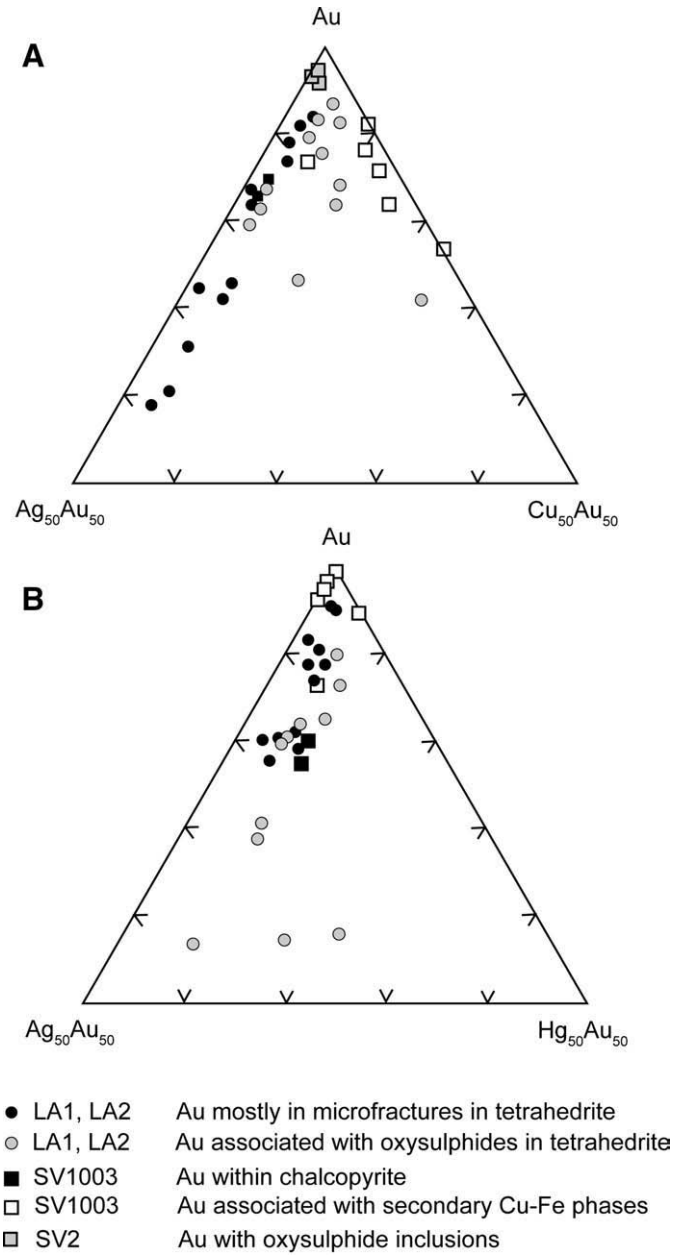

Fig. 2. Triangular Au–Ag–Cu and Au–Ag–Hg compositional plots showing the composition of native gold from Larzenbach (LA1, LA2) and St. Veit im Pongau (SV1003, SV2).

Please cite this article as: Kucha, H., Raith, J.G., Gold-oxysulphides in copper deposits of the Greywacke Zone, Austria: A mineral chemical and infrared fluid inclusion study, Ore Geology Reviews (2008), doi:10.1016/j.oregeorev.2008.10.004

samples from Larzenbach is lower (Sb/(Sb+As)=0.83 to 0.88) compared to those from St. Veit (0.93 to 0.95). In contrast the St. Veit samples are richer in Zn (Table 1). Tetrahedrite is converted into tennantite only around microfractures carrying gold inclusions (Table 1; analysis LA2 A11, Sb/(Sb+As)=0.02). Previously published microprobe traverses across microfractures containing gold show that the tetrahedrite close to the microfractures is in addition to As also enriched in Zn and Ag but depleted in Fe and Hg (Kucha et al., 1997b).

Tetrahedrite contains inclusions of cubanite, chalcopyrite, talnakhite, pyrite, arsenopyrite, gersdorffite, ullmanite, saffloritе–löllingite–rammelsbergite, galena, gold, graphite and the gangue minerals quartz, muscovite, and calcite. Cuprite, covellite and limonite formed during supergene alteration of the sulphide ores. Tetrahedrite is crosscut by multiple fractures and microfractures. Minerals identified in microfractures within tetrahedrite include native gold and gold-oxysulphides (see Section 5.3), chalcopyrite, talnakhite, haycockite, arsenopyrite, pyrite, cuprite, malachite, gersdorffite, ullmanite and rare tennantite (see above).

5.2. Gold

Trace element contents analysed on hand-picked sulphide-rich bulk samples from Veitsch and Mitterberg were previously published (Kucha et al., 1995, 1997b). In massive tetrahedrite, Au ranges from (in ppm) 5 to 52.5, Ag from 350 to 1320, and Pb from 67 to 350; Pt and Pd contents are at the few ppb level. The gold content of massive chalcopyrite is much lower; it ranges from 0.3 to 1.5 ppm Au. Native gold occurring in tetrahedrite varies in size from a few to 250 µm. Most of the visible gold is found within and close to microfractures within tetrahedrite. The remaining visible gold is intergrown with or encapsulated by sulphoarsenides (mainly arsenopyrite) and often contains large amounts of low reflectance Au-oxysulphides.

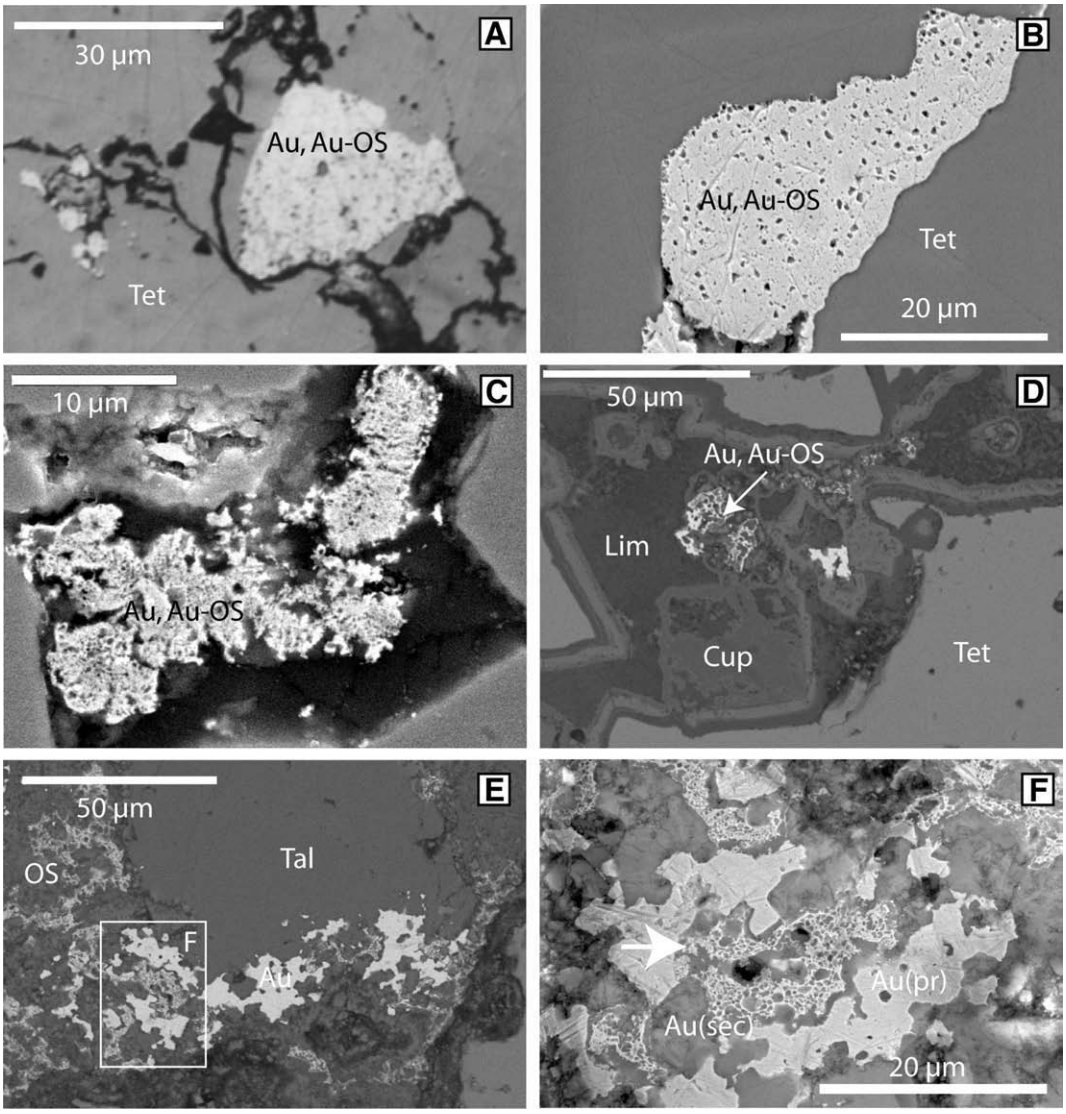

Fig. 3. Reflected light microphotograph (A) and secondary electron images (B–F). A. Gold (Au) with minute inclusions of gold-oxysulphides (Au-OS) in tetrahedrite (Tet); sample SV4 St. Veit. B. Native gold (Au) with a myriad of inclusions of Type 1 gold oxysulphides (Au-OS) in tetrahedrite (Tet); sample SV2, St. Veit im Pongau. C. Complex intergrowths of spongy gold with dark inclusions of Type 1 gold oxysulphides; sample LA1, Larzenbach/Hüttau. D. Native gold and Type-2 gold oxysulphides (Au, Au-OS) with limonite (Lim) and cuprite (Cup); sample SV1003, St. Veit im Pongau. E. Native gold, Cu–Fe-oxysulphides (OS) and talnakhite (tal); sample SV1003, St. Veit im Pongau. F. Detail of E (field-emission SEM image) showing inclusion-free primary gold (Au (pr)) and spongy, Cu-rich secondary gold (Au (sec)); the latter is intergrown with dark Type 2 oxysulphides; arrow points out replacement of primary gold by secondary gold plus gold oxysulphides.

Please cite this article as: Kucha, H., Raith, J.G., Gold-oxysulphides in copper deposits of the Greywacke Zone, Austria: A mineral chemical and infrared fluid inclusion study, Ore Geology Reviews (2008), doi:10.1016/j.oregeorev.2008.10.004

Analyses of gold from Larzenbach and St. Veit are listed in Table 2 and shown in Fig. 2. Gold composition as determined by electron microprobe depends on the mineral assemblage in which gold occurs (Kucha et al., 1995, 1997a,b, 2003). Six types of gold can be distinguished in the Greywacke Zone:

1. Primary (?) gold is present in massive, non-fractured tetrahedrite. This gold usually forms grains from a few to rarely 20 μm. At Larzenbach and St. Veit these primary gold inclusions were too small to obtain high-quality analyses. The average composition (n = 10 measurements, wt.%) of this type of gold from Veitsch and Mitterberg is: Ag 25.18, Au 67.39, and Hg 7.05. The Cu content is below detection limit (Kucha et al., 1995, 1997a).
2. Native gold and electrum present within microfractures in tetrahedrite together with pyrite, gersdorffite, chalcopyrite, cubanite, arsenopyrite and quartz. This gold is free of oxysulphide inclusions. The finest gold occurs together with Cu–As-bearing pyrite replacing tetrahedrite. Ag-rich gold is associated with quartz inclusions. At Larzenbach microfracture-hosted gold in tetrahedrite is Ag- and Hg-rich (9.44 to 25.59 wt.% Ag, 4.58 to 21.25 wt.% Hg), and contains 1.05 to 3.88 wt.% Cu (Table 2). Composition of chalcopyrite-hosted gold from St. Veit is similar to that in tetrahedrite microfractures (SV1003 B2, B3, Table 2). At Mitterberg the Cu content in this gold is usually between ≤0.06 and 2.0 wt.% and the Hg concentration varies from ≤0.09 to 9.80 wt.% (Kucha et al., 1997a). Arsenopyrite-hosted gold from St. Veit im Pongau, Teufelrauchfang (SV2 B3–B5), contains 0.34–1.07 wt.% Cu and has some Ag (2.34 to 3.02 wt.%, Table 2). At Mitterberg this type of gold is enriched in (wt.%) Cu 3.73 to 4.94, and Sb 3.17 to 4.44 but has very low contents of Ag (≤0.03 to 0.14) and Hg (≤0.03 to 0.21; Kucha et al., 1997a).
3. An unnamed Ag_2Au_3Hg phase occurs in fractures in tetrahedrite at Mitterberg either as solitary grains or together with a second generation of chalcopyrite or gersdorffite. It represents probably a new mineral (Kucha et al., 1997a). This new Ag_2Au_3Hg phase has a different chemical formula than weishanite $(Au,Ag)_3Hg_2$ and it is optically isotropic while weishanite is weakly anisotropic. Weishanite has significantly higher reflectance of 76.3% at 534 nm, and 81.3% at 589 nm, while for the new Ag_2Au_3Hg phase R% for these wavelengths is 59.2 and 69.7, respectively. Therefore chemical composition and optical properties clearly distinguish the found Ag_2Au_3Hg phase from weishanite.
4. Gold intergrown with oxysulphides of Type 1 (see Section 5.3) from the hydrothermal paragenesis. This type of gold has a weak pink hue in reflected light and is spotted with μm-size dark inclusions of oxysulphides (Fig. 3A–D). At Larzenbach this type of gold (LA2 A1, A5, A6, A10; LA2 D7; Table 2) has (in wt.%) 5.55 to 16.97 Ag, 1.26 to 6.57 Hg, 2.13 to 2.91 Cu and up to 1.78 Sb. In addition two analyses have higher As contents (LA1 D4, D5, Table 2).
5. Gold from the supergene weathering paragenesis is characterised by the highest Cu contents (4.6 to 22.07 wt.%, Fig. 2, Table 2). In reflected light this secondary gold has a strong pink hue and is intergrown with oxysulphides of Type 2 (Section 5.3, Fig. 3E, F), cuprite, limonite and less often malachite. It is variable in Ag (<0.06 to 14.87 wt.%), Hg (<0.06 to 4.68) and can contain considerable amounts of Sb (1.04 to 15.73) and minor amounts of S, Fe, and As. The source of this Cu-rich gold is earlier gold present as inclusions in chalcopyrite or talnakhite (Fig. 3F).
6. Refractory gold. Concentrations of invisible gold are up to 0.54 wt.% in tetrahedrite and up to 4.60 wt.% in tennantite (Table 1). Gold valence measured by microprobe in Au-richer microareas within tetrahedrite is 0 (normalised Au Mβ/Mα = 0.8009 ± 0.0022), suggesting that gold is present as sub-microscopic inclusions of native gold. The highest gold concentrations are associated with strong, local enrichment in As in the surrounding tetrahedrite matrix (Table 1, LA2 A11). Cu–As-pyrite present in fractures in tetrahedrite shows two groups of Au Mβ/Mα ratios — one close to 0.8010 ± 0.0027 suggesting valence 0 connected with submicroscopic inclusions of metallic gold, and another close to 0.8079 ± 0.0022 suggesting valence +1 and therefore chemically bound to the host lattice.

5.3. Oxysulphides

Textural relations of oxysulphides to gold and other minerals are illustrated in Fig. 3, representative analyses are listed in Table 3. Under crossed polars oxysulphides show a weak optical anisotropy discernible at grain boundaries with colours of variable brightness and greenish hue. In plain polarised light they are grey with a weak brownish hue. Oxysulphides with submicroscopic exsolutions of gold show yellow-brownish hue. No internal reflections have been observed so far.

Two types of oxysulphides are distinguished: Type 1 oxysulphides are associated with primary gold and preserved as inclusions in gold and in microfractures within tetrahedrite. These oxysulphides are intergrown with native gold of high fineness and rarely occur together with haycockite, chalcopyrite, ullmanite and arsenopyrite. They are also present as myriads of rounded inclusions within larger gold grains (up to 250 μm) enveloped by arsenopyrite and encapsulated in tetrahedrite.

Table 3
Chemical composition of gold-oxysulphides from Larzenbach, Salzburg Province, Austria

	LA2 A2	LA2 A4	LA2 A3a	LA2 A2c	LA2 A2d	LA2 A2e	LA2 A2f	LA2 A2g
wt.%	Oxysulph. 1	Oxysulph. 1	Oxysulph. 2	Oxysulph. 2	Oxysulph. 1	Oxysulph. 1	Oxysulph. 1	Oxysulph. 1
Au	44.09	31.87	10.22	6.95	43.61	41.40	36.41	37.55
Ag	4.03	7.25	1.83	2.74	4.19	4.21	4.18	4.35
Cu	8.21	14.40	22.02	24.77	7.93	7.73	11.22	12.01
Hg	2.90	12.75	3.13	2.50	3.01	2.55	3.22	0.98
Fe	2.17	3.01	1.18	1.50	2.11	1.67	2.25	2.16
Sb	3.56	6.19	12.40	12.79	3.43	2.41	6.51	7.51
S	6.07	11.60	19.17	18.02	8.72	7.30	11.84	13.11
Total	71.03	87.07	69.95	69.94	73.00	67.47	75.63	77.67
O diff	28.97	15.94	30.05	30.06	27.00	32.53	24.37	22.33
mol.								
Au	0.224	0.162	0.052	0.035	0.221	0.210	0.185	0.190
Ag	0.037	0.067	0.017	0.025	0.039	0.039	0.039	0.040
Cu	0.129	0.227	0.347	0.390	0.287	0.122	0.177	0.189
Hg	0.014	0.063	0.016	0.013	0.015	0.013	0.016	0.005
Fe	0.039	0.054	0.021	0.027	0.038	0.030	0.385	0.039
S	0.189	0.361	0.598	0.562	0.272	0.228	0.369	0.409
O diff	1.811	0.808	1.878	1.879	1.688	2.033	1.523	1.396

Oxysulph. 1 and 2 refers to the two types of oxysulphides distinguished (see Section 5.3).
O diff. — oxygen by difference to 100 wt.%.

Please cite this article as: Kucha, H., Raith, J.G., Gold-oxysulphides in copper deposits of the Greywacke Zone, Austria: A mineral chemical and infrared fluid inclusion study, Ore Geology Reviews (2008), doi:10.1016/j.oregeorev.2008.10.004

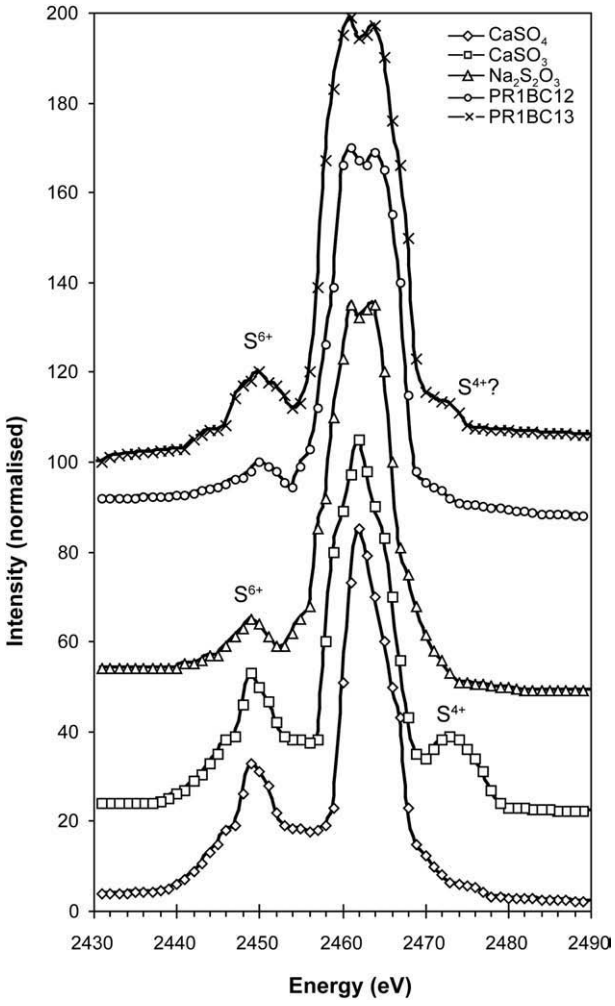

Fig. 4. Scans of the SK_β line in sample PR1BC (PR1BC12 and PR1BC13) from Mitterberg and in standards of known sulphur valence (anhydrite $CaSO_4$: valence=+6, synthetic $CaSO_3$: valence=+4; sodium thiosulphate $Na_2S_2O_3$: valences=+6 and −2, average valence=+2). Note the peak splitting in sample PR1BC, which is typical for compounds of mixed sulphur valence. In scan 13 a weak S^{4+} satellite peak is indicated at ~2472–2476 eV in addition to the diagnostic S^{6+} satellite peak at ~2450 eV. The curves are normalised to 100 intensity units; for clarity they are displaced.

Oxysulphides of Type 1 are *not* interconnected along microfractures in gold but are present as *isolated* solid inclusions (Fig. 3A,C). This observation indicates that Type 1 oxysulphides precipitated coevally with the hydrothermal gold (Type 4 gold, see Section 5.2). Type 1 oxysulphides from Larzenbach have (wt.%): Au 31.87 to 44.09, Cu 7.73 to 14.40, Ag 4.03 to 7.25, Fe 1.67 to 3.01, Sb 2.41 to 7.51 and S 6.07 to 13.11 (Table 3); they are quite variable in Hg (0.98 to 12.75). For comparison, oxysulphides from Mitterberg have (in wt.%): Au 40.11 to 44.20, Cu 14.07 to 24.06, Sb 3.11 to 3.59, and S 15.40 to 18.31 (Kucha et al., 1997b, 2003).

The sulphur valence determinations on oxysulphides by electron microprobe clearly indicate the presence of mixed sulphur valences in these compounds. Similar to the $Na_2S_2O_3$ reference material they show splitting of the main SK_β peak between 2455 and 2470 eV indicating the presence of sulphur +6 and −2 (Fig. 4). Moreover, they show characteristic satellite peaks indicative of S^{6+}. The S^{6+} satellite peak in these oxysulphides is either slightly higher (PR1BC13) or slightly lower (PR1B3C12) than in the $Na_2S_2O_3$ reference material.

Type 2 oxysulphides formed during weathering of tetrahedrite-rich ores and are associated with cuprite, limonite and, less often, malachite. They are associated with secondary gold. It is important to note that in this supergene paragenesis, oxysulphide grains are interconnected (Fig. 3E,F) and the textures indicate local dissolution and re-precipitation of gold (Fig. 3F). During this process the size of the secondary gold grains has increased. Native gold associated with Type 2 oxysulphides has a high Cu content (Table 2, Fig. 2). Oxysulphides of Type 2 are lower in gold and contain (in wt.%) Au 6.95 to 10.22, Cu 22.02 to 24.77, Ag 1.83 to 2.74, Sb 12.40 to 12.79, and S 18.02 to 19.17. Actually they could be oxysulphide–oxyantimonide compounds (Table 3, LA2 A3a, LA2 A2c).

Spectral reflectance measurements for oxysulphides of Type 1 are presented in Fig. 5. Gold–copper oxysulphides (curve PR1B4 A4) are characterised by low reflectance throughout the spectral range (10 to 15%) and flat convex spectral curves. Reflectance increases dramatically in the 520 to 680 nm range when nanometre-sized inclusions of gold are present in the oxysulphides (curve PR1B4 A18).

6. Fluid inclusions

6.1. Transparency of tetrahedrite in infrared light

Infrared microthermometry is an established but not widely used method allowing study of fluid inclusions in some ore minerals, which are opaque in visible light (e.g., Lueders 1996). In the spectral range $\lambda \leq 2.5$ μm some oxides (e.g., wolframite, hematite) and some

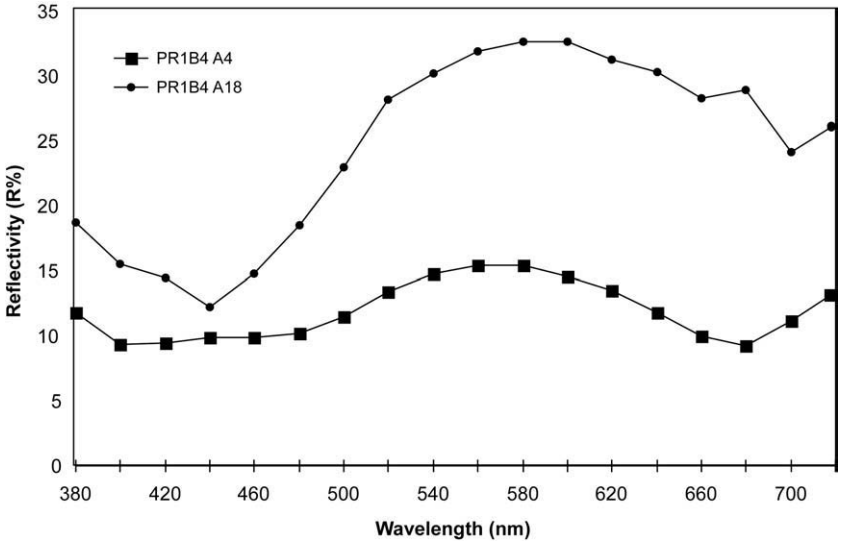

Fig. 5. Spectral reflectance curves (in *R*%) of gold–copper oxysulphides (PR1B4–A4, lower curve) from Mitterberg. These compounds are characterised by low reflectance throughout the spectral range. PR1B4-A18 shows much higher reflectance due to presence of nanometre-sized gold inclusions in the oxysulphides.

Please cite this article as: Kucha, H., Raith, J.G., Gold-oxysulphides in copper deposits of the Greywacke Zone, Austria: A mineral chemical and infrared fluid inclusion study, Ore Geology Reviews (2008), doi:10.1016/j.oregeorev.2008.10.004

sulphides (e.g., stibnite, sphalerite, to some extent pyrite etc.) become transparent (Campbell and Robinson-Cook, 1987; Lueders, 1996; Lueders et al., 1999; Bailly et al., 2000, 2002; Kouzmanov et al., 2002). IR microthermometry has not been widely applied for studying members of the tetrahedrite–tennantite series mostly because their IR-transparency is limited by chemical composition; only As-poor tetrahedrite is IR-transparent whereas tennantite remains opaque also in the IR spectral range (Lueders, personal communication).

Our combined IR and mineral chemical study confirmed that IR transparency is restricted to As-poor tetrahedrite. Tetrahedrite from St. Veit is more transparent than that from Larzenbach reflecting the lower As content in the former (Table 1). The approximate As content where tetrahedrite becomes IR-opaque is ca. 2 to 2.5 wt.% As. Higher As contents cause rapid increase in opacity. In addition, it was observed that temperature has a significant reversible effect on tetrahedrite transparency, i.e., above ~120 °C the opacity of tetrahedrite containing about 2 wt.% As increases significantly making precise microthermometric measurements impossible. Transparency is immediately recovered when temperature drops below ~120 °C.

6.2. Tetrahedrite microtextures

Due to the opacity of arseniferous tetrahedrite the system of microfractures developed in tetrahedrite can be made visible in infrared light (Fig. 6A,E). Under smaller magnification a complex fracture network including larger cracks several tens of μm thick, as well as thin microfractures are to be seen (Fig. 6A,B,E). Small microfractures may coalesce to produce semi-massive dark areas of opaque arseniferous

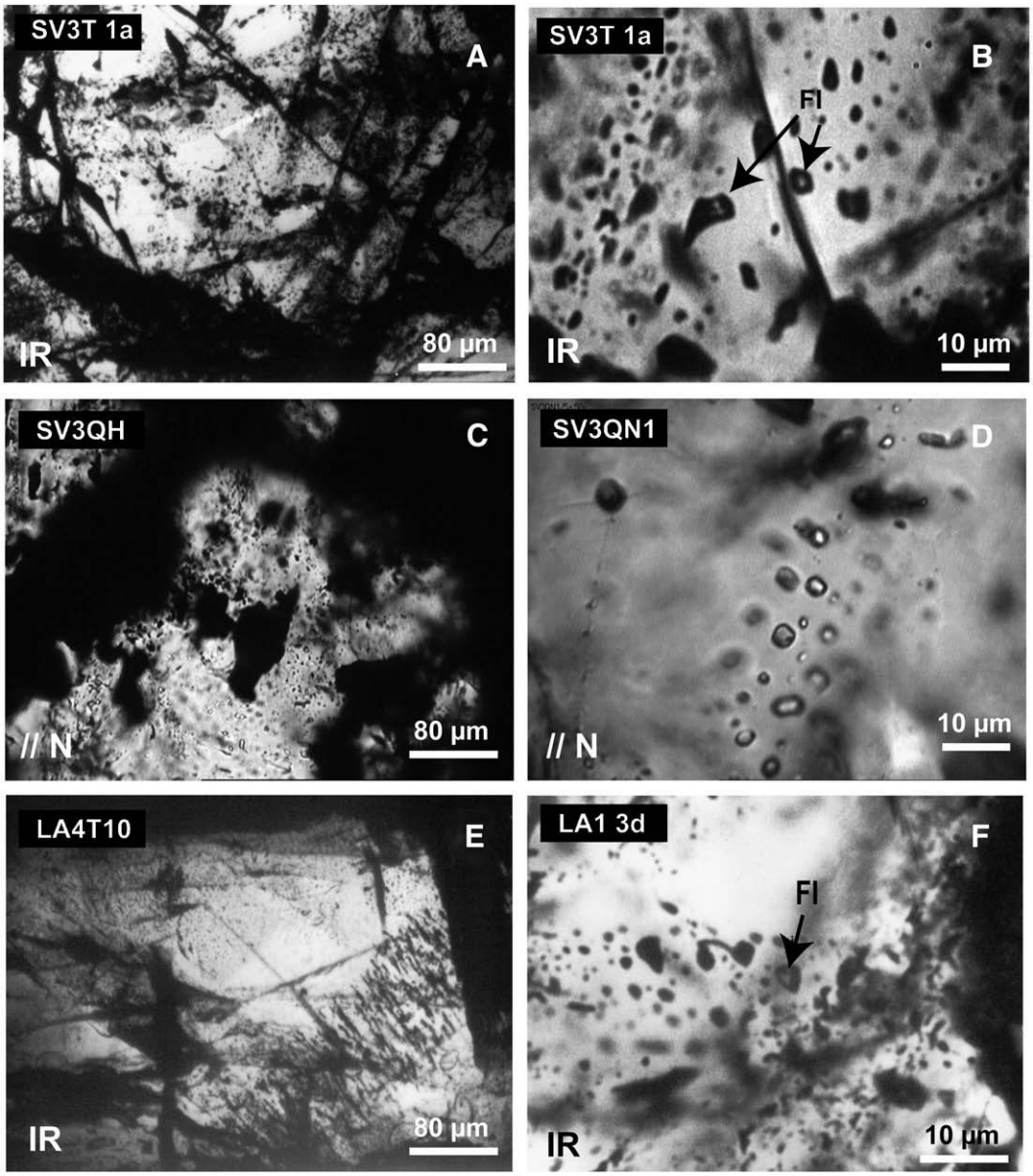

Fig. 6. Microphotographs illustrating microfracturing in tetrahedrite and fluid inclusions in tetrahedrite and quartz. A, B. Infrared (IR) photographs showing IR-transparent tetrahedrite. The microfractures are filled with arseniferous tetrahedrite, which is opaque in the near IR spectral range. The cloudy domains within tetrahedrite are rich in solid and fluid inclusions. B. IR-microphotograph showing details of A. Aqueous two-phase (L+V) fluid inclusions (arrows, FI) within tetrahedrite are of low salinity and represent the Au transporting fluid. Sample SV3, St. Veit im Pongau. C. Transparent quartz intergrown with opaque tetrahedrite. Quartz is rich in opaque solid and aqueous fluid inclusions. D. Trail of aqueous two-phase (L+V) fluid inclusions in quartz. These inclusions represent the higher saline fluids unrelated to Au mineralisation. Sample SV3, St. Veit im Pongau; C and D normal polarised light. E. IR photograph showing in part crystallographically controlled IR-opaque microfractures in tetrahedrite. Sample LA4, Larzenbach. F. IR-microphotograph showing aqueous two-phase L+V fluid (arrow, FI) and opaque solid inclusions in tetrahedrite. Sample LA1, Larzenbach.

Please cite this article as: Kucha, H., Raith, J.G., Gold-oxysulphides in copper deposits of the Greywacke Zone, Austria: A mineral chemical and infrared fluid inclusion study, Ore Geology Reviews (2008), doi:10.1016/j.oregeorev.2008.10.004

Table 4
Summary of microthermometric measurements and calculations of fluid properties for fluid inclusions from Larzenbach (LA1) and St. Veit im Pongau (SV3), Salzburg Province, Austria

	T_h (°C)	T_m (°C)	Density (g/cc)	Mass % NaCl eq
LA1 tetrahedrite				
Mean	122.0	−5.1	0.9875	8.08
Std. dev.	35.6	1.9	0.0322	2.64
Min.	85.0	−8.5	0.9168	4.96
Max.	190.0	−3.0	1.0370	12.28
Points	10	11	10	10
SV3 tetrahedrite				
Mean	165.1	−6.5	0.9678	9.44
Std. dev.	12.8	3.8	0.0341	4.55
Min.	140.0	−14.0	0.9356	4.96
Max.	185.0	−3.0	1.0280	17.79
Points	11	10	10	10
SV 3 quartz, low salinity inclusions (T_m > −10)				$CaCl_2$ eq
Mean	108.0	−6.0	1.0482	9.91
Std. dev.	3.3	2.2	0.0324	2.58
Min.	72.0	−10.0	1.0050	5.95
Max.	157.0	−3.0	1.1110	14.18
Points	8	8	8	8
SV 3 quartz, high salinity inclusions (T_m < −10)				
Mean	104.6	−23.1	1.1375	20.67
Std. dev.	20.5	7.7	0.0244	2.64
Min.	60.0	−44.0	1.1020	17.45
Max.	150.0	−14.5	1.2110	28.96
Points	25	24	24	24

Microthermometric data for tetrahedrite were obtained using IR-microthermometry. T_h total homogenisation temperature, T_m final ice melting temperature.

tetrahedrite (Fig. 6E). Under higher (~600×) magnification fluid inclusions can be observed in vicinity of these opaque microfractures (Fig. 6B,F). In addition some (micro)fractures contain black, IR-opaque solid inclusions (Fig. 6B,F) that were identified in reflected light mainly as chalcopyrite, gold and Type 1 oxysulphides.

Tetrahedrite from Larzenbach has a similar system of fractures and microfractures controlling replacement of tetrahedrite by arseniferous tetrahedrite, but it also shows larger areas spotted with small inclusions of finely dispersed arseniferous tetrahedrite; these elongate inclusions are partly interconnected and seem to be crystallographically controlled, e.g., by cleavage planes (Fig. 6E).

6.3. Fluid inclusions in tetrahedrite

Fluid inclusions in tetrahedrite were observed close to microfractures (Fig. 6A,B,F). They are usually accompanied by myriads of small solid, opaque inclusions of chalcopyrite, minor arsenopyrite and rarely oxysulphides and gold (Fig. 6B,F). Presence of these minerals has been confirmed by reflected light microscopy and SEM studies on polished surfaces of tetrahedrite containing fluid inclusions.

Fluid inclusions from tetrahedrite sample SV3 St. Veit are of irregular shape and commonly smaller than 10 μm. They occur as individual inclusions but mostly along trails (Fig. 6B); at least the latter must be of secondary origin. The inclusions are two-phase aqueous inclusions containing a liquid (L) and a vapour (V) phase and homogenise into the liquid phase (V→L). Within a single trail they show consistent L:V ratios (estimated L:V=70:30). Fluid inclusions of sample SV3 yielded temperatures of homogenisation (T_h) between 140 and 185 °C (Table 4; Fig. 7). Temperatures of final ice melting (T_m) vary between −3 to −14 °C and indicate fluids of low to moderate salinity (Table 4, Fig. 7).

Fluid inclusions in tetrahedrite sample LA1 from Larzenbach are of irregular to rounded shape. They occur in clusters and as small (<10 μm) isolated inclusions together with opaque solid inclusions (Fig. 6F). Because of the small inclusion size estimation of the L:V ratio is difficult but it seems to be less consistent than in sample SV3; T_h (V→L) ranges between 85 and 190 °C, T_m between −3 to −8.5 °C (Table 4, Fig. 7).

6.4. Fluid inclusions in quartz

Fluid inclusions in quartz are much more common than in tetrahedrite; these were studied in normal visible light in sample

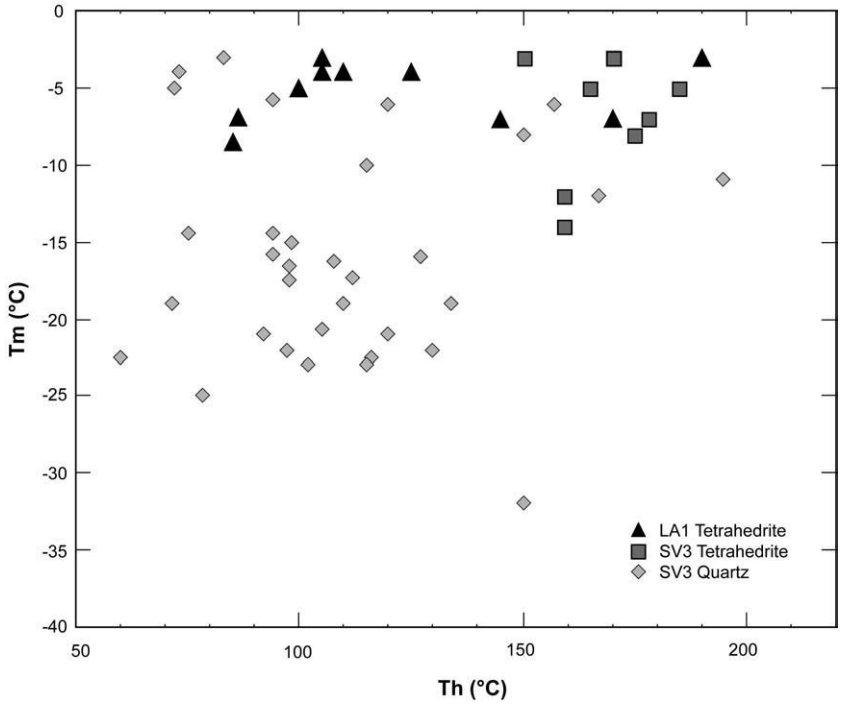

Fig. 7. Plot of temperature of homogenisation (T_h) versus temperature of final ice melting (T_m) for fluid inclusions in tetrahedrite and quartz from Larzenbach and St. Veit im Pongau. Aqueous fluids of low salinity were found in tetrahedrite and quartz. Higher saline (lower T_m) aqueous fluids, unrelated to Au mineralisation, are restricted to quartz.

Please cite this article as: Kucha, H., Raith, J.G., Gold-oxysulphides in copper deposits of the Greywacke Zone, Austria: A mineral chemical and infrared fluid inclusion study, Ore Geology Reviews (2008), doi:10.1016/j.oregeorev.2008.10.004

SV3 from St. Veit in which two types of fluid inclusions in quartz are distinguished:

Quartz Type 1 (lower salinity). The occurrence of many small fluid inclusions in quartz, which is intimately intergrown with As-poor tetrahedrite, may give the latter a clouded appearance in transmitted light (Fig. 6C). These fluid inclusions occur in clusters rather than in trails, are of irregular to rounded shape, and small (<5 μm). They are aqueous two-phase (L+V) to one-phase (? L) and have variable L:V ratios. T_h (V→L) of individual two-phase inclusions within this cluster varies considerably (72 to 195 °C; with one outlier at 250 °C); T_m for FI Type 1 inclusions ranges from −3 to −12 °C.

Quartz Type 2 (higher salinity). The majority of fluid inclusions in quartz, however, are of higher salinity (T_m down to −44 °C) and homogenise at lower temperatures (60 to 150 °C; Table 4, Fig. 7). These inclusions are not directly related to tetrahedrite. These aqueous two-phase inclusions are small (<5 to 10 μm) show consistent L:V (90:10) ratios and preferentially occur along secondary inclusion trails (Fig. 6D). Larger (c. 10 μm) solitary fluid inclusions of irregular shape are irregularly distributed in quartz. They are aqueous two-phase (L+V) inclusions and always show large and well visible gas bubbles. These larger inclusions have high salinity and T_h between 120 and 150 °C. Low eutectic temperatures T_e (e.g., quite consistently below c. −56 °C) and the observation of final ice melting between −36.5 and −32 °C suggest that in addition to NaCl, there are other salts ($MgCl_2$?) present in the fluid.

7. Discussion

7.1. Fluid composition and origin

The gold mineralising fluids entrapped in tetrahedrite are characterised as moderately saline aqueous solutions. The salinities (T_m) show considerable overlap with lower salinity (Type 1) fluid inclusions in quartz although the latter show slightly lower mean T_h and higher densities (Table 4). The fluid inclusions in tetrahedrite are preferentially found along microfractures healed by arseniferous tetrahedrite and are associated with gold encapsulating solid inclusions of gold-oxysulphides. From textural relationships it is, therefore, concluded that formation of native gold with inclusions of Au-oxysulphides is related to these low-salinity fluids. Obviously gold mineralisation is not related to the high-salinity fluids entrapped in Type 2 fluid inclusions in quartz, which have comparable range in T_h but much lower T_m values.

Previous studies of fluid inclusions from the main vein of the Mitterberg Cu deposit (part of the same ore district as Larzenbach and St. Veit) demonstrated the presence of several populations of aqueous fluids with high salinity in this deposit (Belocky, 1992; Pohl and Belocky, 1999). Highly saline halite-saturated (L+V+halite±calcite, T_h 127±38, 26 to 38 wt.% NaCl equiv.) brines evolve to saline halite-undersaturated (L+V; T_h ~100 °C, 21 to 23 wt.% NaCl equiv.) fluids. Formation conditions deduced for L+V+halite inclusions were >240 °C and ≥200 MPa. Interestingly, these inclusions never contain CO_2 as a separate phase at room temperature. These CO_2-free aqueous brines were interpreted as syn-orogenic fluids that are characteristic for Eoalpine ore deposits in the Eastern Alps formed during the Cretaceous ("syn-orogenic Austroalpine fluid province" of Pohl and Belocky, 1999).

When comparing our data with those published by Belocky (1992) it can be seen that higher salinity inclusions in quartz from St. Veit (SV3) correspond to the saline halite-undersaturated population of Belocky (1992). The low to moderately saline fluids that we document from tetrahedrite and quartz have, however, not been reported before. It is important to note that gold mineralisation in the copper deposits of the Greywacke Zone is related to this *latter* fluid type and not to the syn-metamorphic highly saline brines, which were interpreted to have formed by de-volatilisation of crustal rocks likely involving evaporitic sequences during Eoalpine subduction and collision of Penninic underneath Austroalpine tectonic units (Pohl and Belocky, 1999).

The gold mineralising fluids in the polymetallic Cu deposits of the Greywacke Zone also differ significantly from those observed in Neoalpine mesothermal vein type gold deposits in the Alps (Belocky, 1992; Horner et al., 1997; Pettke et al., 2000) and world-wide (Ridley and Diamond, 2000); in these low-salinity mixed aqueous-carbonic fluids predominate. Hence, *compositionally* gold mineralising fluids in the Greywacke Zone do not resemble syn-metamorphic fluids formed during devolatilisation of deeper crustal rocks during Eoalpine regional metamorphism or late orogenic fluids involved in formation of Neoalpine gold–quartz veins in the Alps.

On the other hand there are field and textural arguments suggesting that formation of gold mineralisation in the copper deposits in the Greywacke Zone must be related to Eoalpine regional metamorphism and deformation. Field relations indicate that Cu (–Au) mineralisation at Mitterberg and at Larzenbach is hosted by discordant as well as concordant veins. Although syngenetic models were proposed for the concordant ore type by some authors (see discussion in Weber, 1997) there is at least agreement that formation of the main discordant copper vein at Mitterberg is of Cretaceous age (Petraschek, 1978). Paragenetic studies at Mitterberg also document that tetrahedrite, now to be recognised as the main host mineral of Au, is a late stage mineral in the ore paragenesis (Bernhard, 1966).

Microtextural evidence presented in this paper supports the view that gold and oxysulphides postdate tetrahedrite formation. Gold was brought into the rocks when the deformation style changed from ductile to brittle as indicated by the control of gold by microfracturing of tetrahedrite. The minimum formation temperatures of this mineralisation event can be deduced from homogenisation temperatures (Larzenbach LA1: 122±36 °C, St. Veit SV3: 165 ±13 °C) of fluid inclusions in tetrahedrite. Using isochores calculated for tetrahedrite-hosted inclusion data and assuming maximum pressures of 200 MPa as deduced for the final stage of mineralisation at Mitterberg (Belocky, 1992) maximum formation temperatures of gold mineralisation are estimated to be <180 to 300 °C for Larzenbach and <250 to 300 °C for St. Veit (Fig. 8). Most likely pressures were below 200 MPa and temperatures during the gold mineralisation stage did not exceed ~250 °C as deduced from the upper stability limit of oxysulphides (Giggenbach, 1974).

In summary, we interpret gold mineralisation in the Greywacke Zone to be related to late to post-orogenic processes. Compared to typical mesothermal orogenic gold deposits (e.g., in the Tauern window) the deduced temperatures are lower and the H_2O–CO_2 dominated fluids are lacking. Gold mineralising fluids in the GWZ are characterised as lower saline aqueous fluids.

7.2. Transport and precipitation of gold

The aqueous speciation, the transport and the precipitation of gold in/from hydrothermal solutions are controlled by many factors, such as solution composition, temperature, pressure, oxidation potential, and pH (Seward, 1984). Chloro- and hydroxochloro-complexes (e.g., $AuCl_2^-$ are important in high temperature hydrothermal fluids with high activity of chlorine and low activity of reduced sulphur species (Henley, 1973; Seward, 1984, 1991; Tossell, 1996; Stefansson and Seward, 2004). At temperatures between 150 to 350 °C with oxidation states buffered by sulphate–sulphide or H_2 at neutral or alkaline pH the dominant Au species will be $Au(HS)_2^-$ (Shenberger and Barnes, 1989). At acidic pH $AuHS^0$ may become an important species in reduced sulphur-containing hydrothermal solutions (Benning and Seward, 1996) whereas in dilute chloride and sulphide solutions gold hydroxo-complexes (e.g., Au(OH) can become important (Stefansson and Seward, 2004).

Reduced hydrosulphido complexes of gold such as $Au(HS)_2^-$ are the most accepted species for transporting gold in the Earth's crust in weakly

Please cite this article as: Kucha, H., Raith, J.G., Gold-oxysulphides in copper deposits of the Greywacke Zone, Austria: A mineral chemical and infrared fluid inclusion study, Ore Geology Reviews (2008), doi:10.1016/j.oregeorev.2008.10.004

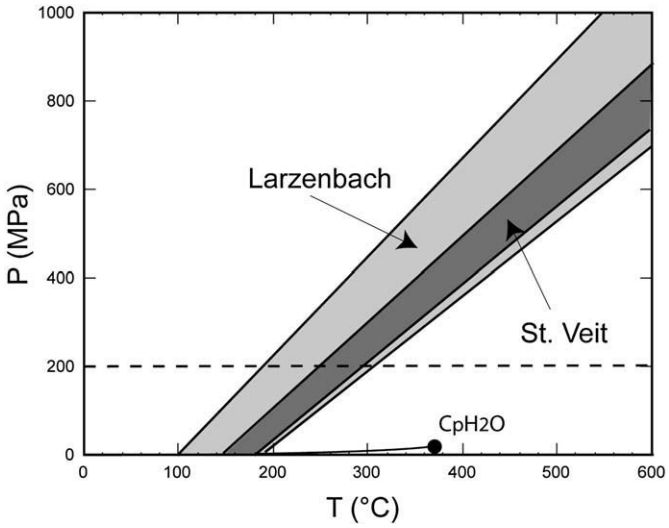

Fig. 8. Pressure–temperature diagram showing calculated range of isochores for tetrahedrite-hosted fluid inclusions from Larzenbach and St. Veit im Pongau. The dashed line constrains the upper pressure limit deduced for fluid inclusion entrapment at Mitterberg (according to Belocky, 1992).

acidic to neutral and reduced meso- to epithermal fluids. However, in low-temperature fluids with higher oxidation potential gold can also combine with oxoacids of sulphur such as thiosulphate ($S_2O_3^{2-}$) or polythionates ($S_nO_6^{2-}$), and sulphite (SO_3^{2}) (Seward, 1991), in which sulphur is in an intermediate oxidation state between −2 and +6. Experimental work by Berndt et al. (1994) showed that polysulphides (S_nS^{2-}) of the type AuS_nS^{1-}, where $n=2$ to 7, play a significant role in gold transport and deposition of gold at low temperatures (100 to 150 °C) in fluids close to sulphur saturation.

The close association of gold with oxysulphides, as documented for some vein-type gold deposits in eastern Australia and South Africa, has been used as argument for the transport of gold by thiosulphate complexes in the low-temperature (<250 °C) hydrothermal regime (Kucha et al., 1994). The presence of thiosulphate among the anionic species analysed in fluid inclusions from the Omai gold deposit, Guyana, also supports the importance of thiosulphate complexing of gold in some vein-type gold deposits (Voicu and Hallbauer, 2005).

P–T–X conditions suitable for transport of gold as thiosulphate complexes are also to be expected in the upper levels of hydrothermal systems and these species were actually confirmed in hydrothermal fluids from hot springs in Waiotapu, New Zealand (Pope et al., 2005) and Yellowstone, USA (Xu et al., 1998). For the Champagne Pool, Waiotapu, New Zealand, dissolved gold contents up to 109 ng L^{-1} were reported and high gold concentrations (40 to 90 ng L^{-1}) were also noted further downstream in acidified geothermal fluids. These runoff waters are oversaturated with respect to reduced Au–S species and hence Pope et al. (2005) assumed that in these fluids gold is transported by ligands such as polysulphides, thiosulphates or colloid particles.

From the present fluid inclusion study it can be concluded that gold in the Au-bearing Cu deposits of the GWZ was transported by hydrothermal fluids of low salinity that were below ~250 °C. The low activity of chlorine, as documented by the low total salinity of the fluid inclusions, and the temperature constraints of the transporting fluids therefore make the transport of gold by chloro- and hydroxychloro complexes unlikely. Rather, gold sulphur complexes are the preferable species for gold transport.

The presence of gold oxysulphides, i.e., solid compounds of intermediate sulphur valence containing sulphur and oxygen, and their intimate nano- to microscale intergrowth with native gold in the studied occurrences in the GWZ is a strong argument for the transport of gold by oxoacids of sulphur such as gold thiosulphate complexes. Because gold oxysulphides are now documented along 350 km in E–W direction in the GWZ (Fig. 1) we argue that transport and mobilisation of gold by these complexes is not a local phenomenon but must have occurred on a *regional* scale in the Alpine orogen.

Possible processes for precipitating gold from hydrothermal solutions include cooling, fluid immiscibility (e.g., boiling), fluid mixing, changes in fS_2 of the fluid (e.g., by formation of sulphides co-precipitated with the gold), changes of pH and fO_2 (e.g., by interaction with the wall rock) or adsorption of gold on mineral surfaces or colloids; among these processes cooling and boiling are regarded as the most effective ones (e.g., Seward, 1991). Based on the study of fluid inclusions boiling or fluid mixing can, however, be excluded for the GWZ. There is no evidence for heterogeneous fluid entrapment as to be expected for fluids undergoing phase separation during boiling and there is no systematic trend to be seen in the T_m vs. T_h diagram, what would be expected when fluids of different temperature and salinity would have undergone mixing. The large variation in T_h, as documented for the low-salinity fluid inclusion population (e.g., Larzenbach T_h of fluid inclusions in tetrahedrite ranges from ca. 80 to 180 °C; Fig. 7), rather indicates cooling of the hydrothermal fluids making this a viable process for precipitation of gold.

7.3. Association of arsenic and gold

Other aspects that need to be discussed are the close spatial association of gold with tetrahedrite, the higher gold grades of tetrahedrite-rich ores and especially the change of tetrahedrite composition close to the gold containing microfractures. As revealed by bulk rock analyses of sulphide concentrates tetrahedrite has much higher gold content compared to coexisting chalcopyrite (see section 5.2). Moreover, the composition of tetrahedrite changes from As-poor to arseniferous tetrahedrite or even tennantite close to Au-bearing microfractures. From these observations we conclude that there exists a genetic link between arsenic and gold.

The close association between the distribution of gold and arsenic in various types of gold deposits has long been recognised. In sediment-hosted (Carlin-type) gold deposits Au and As are chemically closely associated and gold is commonly hosted in arsenian sulphides (especially arsenian pyrite; Arehart et al., 1993; Fleet and Mumin, 1997; Simon et al., 1999b; Cline, 2001). A similar close association of these two elements is known from some Au-bearing volcanic massive sulphide deposits (e.g., McClenaghan et al., 2004) or active geothermal systems (e.g., Rotokawa, New Zealand; Krupp and Seward, 1987).

Furthermore, arsenic, mostly present as arsenopyrite, is a common element in gold deposits in metamorphic terranes, especially in mesothermal orogenic gold deposits hosted by metasediments (Goldfarb et al., 2005). Some of these deposits, such as the Salsigne deposit, France (Demange et al., 2006), have been major resources of arsenic in addition to gold. Arsenic dominated orogenic gold deposits were also mined in the Eastern Alps. There, structurally controlled mesothermal vein type to replacement As–Au–Ag–(Bi) mineralisation developed in the metamorphic dome complex of the Tauern Window during post-collisional uplift (e.g., Rotgülden area, Austria, Horner et al., 1997).

Although As is not a dominant element in the studied Au-bearing Cu deposits of the Greywacke Zone there is an undeniable association of arsenic and gold even in these deposits. As documented in this study gold and Type 1 gold oxysulphides are preferentially found in microfractures within tetrahedrite. Along and around these re-healed microfractures tetrahedrite is becoming increasingly arseniferous making tetrahedrite non-transparent in the IR spectral range (Fig. 6). To explain this close association of gold and arsenic we have to assume that As was either transported together with Au in the hydrothermal solutions or that As played a key role in scavenging Au by adsorption processes on As-containing sulphide surfaces. Because of the geochemical association of gold with arsenic and antimony, especially in epithermal gold deposits, already Seward (1973) suggested that

Please cite this article as: Kucha, H., Raith, J.G., Gold-oxysulphides in copper deposits of the Greywacke Zone, Austria: A mineral chemical and infrared fluid inclusion study, Ore Geology Reviews (2008), doi:10.1016/j.oregeorev.2008.10.004

"arseniothio and atimonothio complexes [e.g., $Au(AsS_2)^0$, $Au(AsS_3)^{2-}$, $Au(Sb_2S_4)^-$, etc.] may be of importance in the transport of gold in some hydrothermal ore solutions". Adsorption has been identified as an important process for fixing gold on sulphide surfaces and triggering its precipitation from gold-undersaturated solutions (e.g., Arehart et al., 1993; Simon et al., 1999a; Reich et al., 2005).

For the studied Greywacke Zone ores we must assume joint transport of arsenic and gold in the hydrothermal solutions because tetrahedrite from the pre-gold chalcopyrite–tetrahedrite assemblage is quite poor in As (Table 1) whereas it was enriched during the gold forming stage.

Transport of arsenic in natural waters is mainly in the form of oxo-anion complexes where arsenic occurs in the nominal As^{3+} or As^{5+} valence state. Depending on pH and redox conditions the most important aqueous species are either arsenite (e.g., $H_3As^{3+}O_3^0$) or arsenate complexes (e.g., $H_2As^{5+}O_4^-$, $HAs^{5+}O_4^{2-}$, Smedley and Kinniburgh, 2002; O'Day, 2006). At higher concentrations of sulphur in aqueous solutions thioarsenic species (e.g., the thioarsenites $As(SH)_3^0$, $As(OH)(SH)_2^0$ etc.) could become additional important aqueous species (Helz et al., 1995; Wilkin et al., 2003). The confirmation of thioarsenic complexes in geothermal waters in the Yellowstone National Park (Planer-Friedrich et al., 2007) confirms the importance of these species for transport of arsenic in natural hydrothermal fluids; interestingly thiosulphate has been detected in the same samples.

Clarke and Helz (2000) pointed out that thioarsenite anions are very effective in transporting soft cations such as Cu, Ag, and Hg and that in multicomponent systems (e.g., the ternary Cu–As–S system) much higher solubilities of theses metals are reached than in any of the binary subsystems. This is in part due to the effect of formation of stable copper thioarsenite complexes (e.g., $CuH_2AsOS_2^0$). Based on theoretical calculations Tossell (2000) concluded that a similar gold thioarsenite complex (AuH_2AsOS_2) should be quite stable in aqueous solutions containing both sulphur and arsenic. Transport of gold by this (theoretical) complex could explain the association of these elements in many gold deposits.

Transport of gold by such unusual species, in addition to the proposed transport by thiosulphate complexes, is also an attractive hypothesis for the Greywacke Zone. In these gold-bearing polymetallic ore deposits, formed from multicomponent ore fluids, the solubility of gold is expected to increase in the presence of As and Cu. Precipitation of the gold could have occurred through simple cation exchange on tetrahedrite surfaces, created by brittle fracturing, through $AsSb_{-1}$ exchange destabilising the gold thioarsenite complexes and resulting in precipitation of gold. This could have been a complementary process for gold precipitation to simple cooling indicated by fluid inclusions.

7.4. Supergene processes

The second type of Au-oxysulphides (Type 2) must have formed at very low temperatures during supergene alteration, what is indicated by the association of oxysulphides with minerals formed during weathering (e.g., Fe-hydroxides, cuprite) and their co-existence with secondary Cu-rich native gold. Again, using textural criteria (i.e., the intimate intergrowths of oxysulphides and secondary gold; Fig. 3E,F) we conclude that thiosulphate complexes played a major role in formation of the secondary gold.

The importance of thiosulphate ligands for the transport of gold and other elements such as uranium in the supergene zone has been pointed out in several studies (e.g., Granger and Warren, 1969; Webster, 1986; Benedetti and Boulegue, 1991; Bowell et al., 1993). Especially during supergene alteration of carbonate-hosted gold ores the weathering fluids formed are likely to be alkaline and gold complexing by sulphur-bearing ligands is more likely than by chloro-complexes. Under moderately oxidising conditions intermediate oxoacids of sulphur species (e.g., thiosulphate) form and are capable of mobilising and upgrading gold and silver ores (Webster, 1986). In addition to purely inorganic processes bacteria may play a crucial role for destabilising gold thiosulphate complexes and reprecipitation of gold in the supergene zone (Lengke and Southam, 2005).

Transport of gold under supergene conditions by thiosulphate complexes has been discussed for secondary gold enrichment in the supergene zone at the Upper Ridges Mine, Wau, Papua New Guinea, where carbonate-bearing primary gold ores are subjected to weathering under tropical–subtropical climatic conditions (Webster and Mann, 1984). High seasonal annual rainfall, a high regional relief and lateral groundwater flow preventing concentration of ions (especially of chloride) in the groundwater were regarded as factors controlling the speciation of gold. Re-precipitation of gold was governed by redox reactions, e.g., by reaction of the gold thiosulphate complex with manganese dioxide or reduction at the water table. Enrichment of gold in lateritic soils developed above Cu–Au deposits (Carajas region, Brazil, Andrade et al., 1991) and in gossans developed above sulphide-bearing quartz veins (Sao Bartolomeu, central Brazil; de Oliveira and de Oliveira, 2000) was also explained with thiosulphate complexing of gold.

Benedetti and Boulegue (1991) analysed gold and thiosulphate concentrations in stream waters and reported 40 times higher gold concentrations close to weathering zones of Au-bearing sulphide ores. Based on field data and from speciation calculations they concluded that the thiosulphate complex $Au(S_2O_3)_2^{3-}$ is the most likely species for mobilising and transporting gold under supergene conditions. This complex forms according to the schematic reaction

$$1/4O_2 + H^+ + Au^0 + 2S_2O_3^{2-} = Au(S_2O_3)_2^{3-} + 1/2H_2O$$

Weathering of sulphides (tetrahedrite, chalcopyrite) would provide the necessary sulphur.

The observation that both primary gold of hydrothermal origin as well as remobilised gold formed during weathering are intimately intergrown with oxysulphides can be regarded as strong evidence that oxoacids of sulphur played a crucial role in transporting gold in the Au-bearing polymetallic ores of the Greywacke Zone. Remobilisation and re-precipitation of secondary Cu-rich gold must have occurred in the presence of these oxoacids (preferably a Au-thiosulphate complex) as evidenced by the intimate intergrowth of gold with oxysulphide phases. The many inclusions of Type 2 oxysulphides within native gold indicate that oxysulphides could have been the metastable precursor phases of metallic gold, which precipitated during continuing oxidation.

Gold was not the only element mobilised during weathering. At least Cu must also have been mobile as indicated by the Cu-rich composition of the oxysulphides and the Cu enrichment in secondary gold. Leaching experiments have shown that Cu too is soluble in thiosulphate solutions and that Cu ions in thiosulphate solutions even have a catalytic effect in speeding up the dissolution of gold considerably (Aylmore and Muir, 2001). The close spatial association of secondary gold and gold oxysulphides with primary gold might indicate that remobilisation and re-precipitation of gold occurred on a very local (cm–dm?) scale. Bowell et al. (1993) also argued that thiosulphate complexes are mostly causing *local* redistribution of gold (up to the metre scale) in lateritic soils.

In the uppermost metres of soil profiles Eh and pH values show considerable variation and the ground water table is an important redox boundary where Au can be enriched (Webster and Mann, 1984; Bowell et al., 1993). Kinetic barriers are to be overcome by catalytic effects of redox sensitive transition metal ions (Fe^{3+}, Cu^{2+}) or thiobacteria (Benedetti and Boulegue, 1991; Lengke and Southam, 2005).

Weathering of gold-bearing sulphide ores is a very complex open system process and hence we can only speculate about the detailed mechanisms of remobilisation, transport and re-precipitation of gold. Because pH was likely buffered by dissolution of carbonates, which are

Please cite this article as: Kucha, H., Raith, J.G., Gold-oxysulphides in copper deposits of the Greywacke Zone, Austria: A mineral chemical and infrared fluid inclusion study, Ore Geology Reviews (2008), doi:10.1016/j.oregeorev.2008.10.004

common in host rocks of the ore deposits studied, oxidation is regarded as a key process for destabilising the thiosulphate complex and causing precipitation of metallic gold in the studied examples.

8. Conclusions

Our results indicate that infrared microscopy is a valuable tool in studying textural relationships between As-poor tetrahedrite, which is transparent in infrared light and more arseniferous opaque members of the tetrahedrite–tennantite series. Tetrahedrite is transparent for infrared light when arsenic content is below ca. 2.5 wt.% As.

Fluid inclusions in tetrahedrite are coeval with small solid inclusions of chalcopyrite, gold oxysulphides and minor arsenopyrite and gold with oxysulphide inclusions. Fluid inclusions in tetrahedrite are of low to moderate salinity and homogenisation temperatures (=minimum formation temperatures) range between 85 and 190 °C. In quartz a similar type of fluid inclusions was found in addition to more saline aqueous fluids, which are unrelated to gold mineralisation.

Gold-oxysulphides are part of the hydrothermal as well as of the weathering mineral assemblages; in the latter they are associated with Cu-rich secondary gold and minerals formed during supergene alteration. The intimate association of gold and gold-oxysulphides indicates that in the Greywacke Zone gold likely was transported and remobilised by thiosulphate complexes. This study demonstrates that gold-oxysulphides are occurring on a regional to even orogenic scale in the Eastern Alps. Because gold-oxysulphides are easily overlooked phases we believe that they should be much more common in other ore districts. Recognition of these phases is relevant because they could be alternative carriers of gold in various low-temperature ore deposits and are expected to influence the processing and recovery of gold in hydrometallurgical processes.

Acknowledgments

Ing. R. Mrazek, manager of the Larzenbach tourist mine, is thanked for guiding us through the mine and for providing sample material. We thank J. Seiser (deceased) and H. Mühlhans for excellent sample preparation. We are grateful to R. Bakker for assistance with fluid inclusion measurements and calculations. The “Kommission für Grundlagen der Mineralrohstoffforschung” of the Austrian Academy of Sciences (ÖAW) is thanked for financial support of this project through a grant to J.G. Raith.

References

Andrade, W.O., Machesky, M.L., Rose, A.W., 1991. Gold distribution and mobility in the surficial environment, Carajas region, Brazil. Journal of Geochemical Exploration 40, 95–114.

Arehart, G.B., Chryssoulis, S.L., Kesler, S.E., 1993. Gold and arsenic in iron sulfides from sediment-hosted disseminated gold deposits — implications for depositional processes. Economic Geology 88, 171–185.

Aylmore, M.G., Muir, D.M., 2001. Thiosulfate leaching of gold — a review. Minerals Engineering 14, 135–174.

Bailly, L., Bouchot, V., Beny, C., Milesi, J.-P., 2000. Fluid inclusion study of stibnite using infrared microscopy; an example from the Brouzils antimony deposit (Vendee, Armorican Massif, France). Economic Geology 95, 221–226.

Bailly, L., Grancea, L., Kouzmanov, K., 2002. Infrared microthermometry and chemistry of wolframite from the Baia Sprie epithermal deposit, Romania. Economic Geology 97, 415–423.

Bakker, R.J., 2003. Package FLUIDS 1. Computer programs for analysis of fluid inclusion data and for modelling bulk fluid properties. Chemical Geology 194, 3–23.

Basso, R., Lucchetti, G., Paelenzona, A., 1991. Gravegliaite, $MnSO_3{\cdot}3H_2O$, a new mineral from Val Graveglia (northern Appenines, Italy). Zeitschrift für Kristallographie 197, 97–106.

Belocky, R., 1992. Regional vergleichende Untersuchung lagerstättenbildender Fluide in den Ostalpen als Hinweis auf eine mögliche metamorphe Ableitung. Braunschweiger geologisch-paläontologische Dissertationen 14, 103 pp.

Benedetti, M., Boulegue, J., 1991. Mechanism of gold transfer and deposition in a supergene environment. Geochimica et Cosmochimica Acta 55, 1539–1547.

Benning, L.G., Seward, T.M., 1996. Hydrosulphide complexing of Au (I) in hydrothermal solutions from 150–400 °C and 500–1500 bar. Geochimica et Cosmochimica Acta 60, 1849–1871.

Berndt, M.E., Buttram, T., Earley III, D., Seyfried Jr., W.E., 1994. The stability of gold polysulfide complexes in aqueous sulfide solutions; 100 to 150 °C and 100 bars. Geochimica et Cosmochimica Acta 58, 587–594.

Bernhard, J., 1966. Die Mitterberger Kupferkieslagerstätte Erzführung und Tektonik. Jahrbuch der Geologischen Bundesanstalt Wien 109, 3–90.

Böhme, E., 1931. Die Kupfererzgänge von Mitterberg in Salzburg. Gangverhalten und Erzfolge. Archiv für Lagerstättenforschung 49, 1–106.

Bowell, R.J., Foster, R.P., Gize, A.P., 1993. The mobility of gold in tropical rain forest soils. Economic Geology 88, 999–1016.

Campbell, A.R., Robinson-Cook, S., 1987. Infrared fluid inclusion microthermometry on coexisting wolframite and quartz. Economic Geology 82, 1640–1645.

Chesnokov, B., Polyakov, V.O., Biushmakin, A.F., 1987. Bazhenovite $CaS_5{\cdot}CaS_2O_3{\cdot}6Ca(OH)_2{\cdot}20H_2O$ — a new mineral. Zapiski Vsesoiusnogo Mineralnogo Obshchestva 116, 737–743 (in Russian).

Clarke, M.B., Helz, G.R., 2000. Metal-thiometalate transport of biologically active trace elements in sulfidic environments. 1. Experimental evidence for copper thioarsenite complexing. Environmental Science and Technology 34, 1477–1482.

Cline, J.S., 2001. Timing of gold and arsenic sulfide mineral deposition at the Getchell Carlin-type gold deposit, north-central Nevada. Economic Geology 96, 75–89.

Demange, M., Pascal, M.L., Raimbault, L., Armand, J., Forette, M.C., Serment, R., Touil, A., 2006. The Salsigne Au–As–Bi–Ag–Cu deposit, France. Economic Geology 101, 199–234.

de Oliveira, S.M.B., de Oliveira, N.M., 2000. The morphology of gold grains associated with oxidation of sulphide-bearing quartz veins at Sao Bartolomeu, central Brazil. Journal of South American Earth Sciences 13, 217–224.

Ebner, F., 1997. Die geologischen Einheiten Österreichs und ihre Rohstoffe. In: Weber, L. (Ed.), Handbuch der Lagerstätten der Erze, Industrieminerale und Energierohstoffe Österreichs. Archiv für Lagerstättenforschung der Geologischen Bundesanstalt. Wien, pp. 106–118.

Feitzinger, G., 2000. Historische Kupferzeche am Larzenbach Hüttau, Salzburger Land. Unpublished excursion guide, St. Gilgen, Salzburg.

Fleet, M.E., Mumin, A.H., 1997. Gold-bearing arsenian pyrite and marcasite and arsenopyrite from Carlin Trend gold deposits and laboratory synthesis. American Mineralogist 82, 182–193.

Goldfarb, R.J., Baker, T., Dube, B., Groves, D.I., Hart, C.J.R., Gosselin, P., 2005. Distribution, character, and genesis of gold deposits in metamorphic terranes. Economic Geology 100th Anniversary Volume 407–450.

Giggenbach, W.F., 1974. Kinetics of the polysulfide-thiosulfate disproportionation up to 240 °C. Inorganic Chemistry 13, 1730–1733.

Goldhaber, M.B., 1983. Experimental study of metastable sulfur oxyanion formation during pyrite oxidation at pH 6–9 and 30 degrees C. American Journal of Science 283, 193–217.

Granger, H.C., Warren, C.G., 1969. Unstable sulfur compounds and the origin of roll-type uranium deposits. Economic Geology 64, 160–171.

Greenwood, N.N., Earnshaw, A., 1984. Chemistry of the Elements. Pergamon Press, Oxford. 1542 pp.

Günther, W., 1978. Die Kupferkiesbaue der Kupfergewerkschaft Larzenbach bei Hüttau (Fritztal)/Salzburg. Der Aufschluss, Sonderheft 29, 365–372.

Heinisch, H., 1988. Hinweise auf die Existenz eines passiven Kontinentalrandes im Altpaläozoikum der Nördlichen Grauwackenzone Ostalpen. Schweizerische Mineralogische und Petrographische Mitteilungen 68, 407–418.

Helz, G.R., Tossell, J.A., Charnock, J.M., Pattrick, R.A.D., Vaughan, D.J., Garner, D.C., 1995. Oligomerization in As (III) sulfide solutions: theoretical constraints and spectroscopic evidence. Geochimica et Cosmochimica Acta 59, 4591–4604.

Henley, R.W., 1973. Solubility of gold in hydrothermal chloride solutions. Chemical Geology 11, 73–87.

Hentschel, G., Tillmanns, E., Hofmeister, W., 1985. Hannebachite, natural calciumsulfite hemihydrate, $CaSO_3X_{1/2}\,H_2O$. Neues Jahrbuch für Mineralogie, Monatshefte 241–250.

Hoinkes, G., Koller, F., Rantisch, G., Dachs, E., Hoeck, V., Neubauer, F., Schuster, R., 1999. Alpine metamorphism of the Eastern Alps. Schweizerische Mineralogische und Petrographische Mitteilungen 79, 155–181.

Horner, J., Neubauer, F., Paar, W.H., Hansmann, W., Koeppel, V., Robl, K., 1997. Structure, mineralogy, and Pb isotopic composition of the As–Au–Ag deposit Rotgülden, Eastern Alps (Austria); significance for formation of epigenetic ore deposits within metamorphic domes. Mineralium Deposita 32, 555–568.

Kouzmanov, K., Bailly, L., Ramboz, C., Rouer, O., Beny, J.-M., 2002. Morphology, origin and infrared microthermometry of fluid inclusions in pyrite from the Radka epithermal copper deposit, Srednogorie Zone, Bulgaria. Mineralium Deposita 37, 599–613.

Kralik, M., Krumm, H., Schramm, M., 1987. Low grade and very low grade metamorphism in the Northern Calcareous Alps and in the Greywacke Zone; illite crystallinity data and isotopic ages. In: Fluegel, H.W., Faupl, P. (Eds.), Geodynamics of the Eastern Alps. Franz Deuticke, Vienna, Austria, pp. 164–178.

Krupp, R.E., Seward, T.M., 1987. The Rotokawa geothermal system, New Zealand, an active epithermal gold-depositing environment. Economic Geology 82, 1109–1129.

Kucha, H., Barnes, H.L., 1995. Compounds with mixed and intermediate sulfur valences in pyrite from the Amelia Mine, Southwest Wisconsin. Mineralium Deposita 30, 78–81.

Kucha, H., Przylowicz, W., 1999. Noble metals in organic matter and clay-organic matrices, Kupferschiefer, Poland. Economic Geology 94, 1137–1162.

Kucha, H., Wouters, R., Arkens, O., 1989. Determination of sulphur and iron valence by microprobe. Scanning Microscopy International 3, 89–97.

Kucha, H., Stumpfl, E.F., Plimer, I.R., Köck, R., 1994. Gold-pyrite association — result of oxysulphide and polysulphide transport of gold? Transactions of the Institution of Mining and Metallurgy, Section B, Applied Earth Science 103, 197–205.

Kucha, H., Prochaska, W., Stumpfl, E.F., 1995. Deposition and transport of gold by thiosulphates, Veitsch, Austria. Mineralogical Magazine 59, 253–258.

Please cite this article as: Kucha, H., Raith, J.G., Gold-oxysulphides in copper deposits of the Greywacke Zone, Austria: A mineral chemical and infrared fluid inclusion study, Ore Geology Reviews (2008), doi:10.1016/j.oregeorev.2008.10.004

Kucha, H., Osuch, W., Elsen, J., 1996. Viaeneite, $(Fe,Pb)_4S_8O$, a new mineral with mixed sulphur valencies from Engis, Belgium. European Journal of Mineralogy 8, 93–102.

Kucha, H., Prochaska, W., Stumpfl, E.F., 1997a. Tetrahedrite, a novel gold trap and its meaning for gold metallogeny in the Austrian Alps. In: Papunen, H. (Ed.), Mineral Deposits, Research and Exploration. Where do They Meet? Balkema, Rotterdam/ Brookfield, pp. 225–228.

Kucha, H., Stumpfl, E.F., Prochaska, W., 1997b. Au-oxysulphide inclusions in gold and their meaning for gold transport and deposition, Mitterberg, Austria. In: Papunen, H. (Ed.), Mineral Deposits, Research and Exploration. Where do They Meet? Balkema, Rotterdam/Brookfield, pp. 225–228.

Kucha, H., Plimer, I.R., Stumpfl, E.F., 1998. Geochemistry and mineralogy of gold and PGE's in mesothermal and epithermal deposits and their bearing on the metal recovery. Physicochemical Problems of Mineral Processing 32, 7–30.

Kucha, H., Raith, J.G., Stumpfl, E.F., 2003. Au-oxysulphies and their role in gold mobility, Northern Greywacke Zone, Austria. In: Eliopoulos, D.G., et al. (Ed.), Mineral Exploration and Sustainable Development. Millpress, Rotterdam, pp. 989–992.

Lengke, M.F., Southam, G., 2005. The effect of thiosulfate-oxidizing bacteria on the stability of the gold-thiosulfate complex. Geochimica et Cosmochimica Acta 69, 3759–3772.

Lueders, V., 1996. Contribution of infrared microscopy to fluid inclusion studies in some opaque minerals (wolframite, stibnite, bournonite); metallogenic implications. Economic Geology 91, 1462–1468.

Lueders, V., Gutzmer, J., Beukes, N.J., 1999. Fluid inclusion studies in cogenetic hematite, hausmannite, and gangue minerals from high-grade manganese ores in the Kalahari manganese field, South Africa. Economic Geology 94, 589–595.

McClenaghan, S.H., Lentz, D.R., Cabri, L.J., 2004. Abundance and speciation of gold in massive sulfides of the Bathurst Mining Camp, New Brunswick, Canada. Canadian Mineralogist 42, 851–871.

Neubauer, F., Handler, R., Hermann, S., Paulus, G., 1994. Revised lithostratigraphy and structure of the Eastern Graywacke Zone (Eastern Alps). Mitteilungen der Österreichischen Geologischen Gesellschaft 86, 61–74.

O' Day, P.A., 2006. Chemistry and mineralogy of arsenic. Elements 2, 77–83.

Paar, W., Köppel, V., 1978. Die Uranknollen-Paragenese von Mitterberg (Salzburg, Österreich). Neues Jahrbuch für Mineralogie Abhandlungen 131, 254–271.

Paar, W.H., Braithwaite, R.S.W., Chen, T.T., Keller, P., 1984. A new mineral, scotlandite ($PbSO_3$) from Leadhills, Scotland; the first naturally occurring sulphite. Mineralogical Magazine 48, 283–288.

Petraschek, W.E., 1978. Zur Altersbestimmung einiger ostalpiner Erzlagerstätten. Mitteilungen der Österreichischen Geologischen Gesellschaft 68, 79–87.

Pettke, T., Diamond, L.W., Kramers, J.D., 2000. Mesothermal gold lodes in the northwestern Alps; a review of genetic constraints from radiogenic isotopes. European Journal of Mineralogy 12, 213–230.

Planer-Friedrich, B., London, J., McCleskey, R.B., Nordstrom, D.K., Wallschlager, D., 2007. Thioarsenates in geothermal waters of Yellowstone national park: determination, preservation, and geochemical importance. Environmental Science and Technology 41, 5245–5251.

Pohl, W., Belocky, R., 1999. Metamorphism and metallogeny in the Eastern Alps. Mineralium Deposita 34, 614–629.

Pope, J.G., Brown, K.L., McConchie, D.M., 2005. Gold concentrations in springs at Waiotapu, New Zealand: implications for precious metal deposition in geothermal systems. Economic Geology 100, 677–687.

Raith, J.G., Vali, H., 1998. Fibrous chlorite and muscovite from the Kaisersberg graphite mine, Styria, Austria. The Canadian Mineralogist 36, 741–754.

Rantitsch, G., Grogger, W., Teichert, C., Ebner, F., Hofer, C., Maurer, E.-M., Schaffer, B., Toth, M., 2004. Conversion of carbonaceous material to graphite within the Greywacke Zone of the Eastern Alps. International Journal of Earth Sciences 93, 959–973.

Ratschbacher, L., Klima, K., 1985. Übersicht über Geologie und Mineralgehalt in einem Querprofil von Altkristallin zur Kalkalpenbasis (Triebenauer Tauernpass — Flitzenschlucht, Paltental, Steiermark, Österreich). Jahrbuch der Geologischen Bundesanstalt Wien 128, 151–173.

Reich, M., Kesler, S.E., Utsunomiya, S., Palenik, C.S., Chryssoulis, S.L., Ewing, R.C., 2005. Solubility of gold in arsenian pyrite. Geochimica et Cosmochimica Acta 69, 2781–2796.

Ridley, J.R., Diamond, L.W., 2000. Fluid chemistry of orogenic lode gold deposits and implications for genetic models. Reviews in Economic Geology 13, 141–162.

Seward, T.M., 1973. Thio complexes of gold and the transport of gold in hydrothermal ore solutions. Geochimica et Cosmochimica Acta 37, 379–399.

Seward, T.M., 1984. The transport and deposition of gold in hydrothermal systems. In: Foster, R.P. (Ed.), Gold '82. The Geology, Geochemistry and Genesis of Gold Deposits. Balkema, Rotterdam, pp. 165–181.

Seward, T.M., 1991. The hydrothermal geochemistry of gold. In: Foster, R.P. (Ed.), Gold Metallogeny and Exploration. Blackie, London, pp. 37–62.

Shenberger, D.M., Barnes, H.L., 1989. Solubility of gold in aqueous sulfide solutions from 150 to 350 °C. Geochimica et Cosmochimica Acta 53, 269–278.

Simon, G., Huang, H., Penner-Hahn, J.E., Kesler, S.E., Kao, L.-S., 1999a. Oxidation state of gold and arsenic in gold-bearing arsenian pyrite. American Mineralogist 84, 1071–1079.

Simon, G., Kesler, S.E., Chryssoulis, S., 1999b. Geochemistry and textures of gold-bearing arsenian pyrite, Twin Creeks, Nevada; implications for deposition of gold in Carlin-type deposits. Economic Geology 94, 405–421.

Smedley, P.L., Kinniburgh, D.G., 2002. A review of the source, behaviour and distribution of arsenic in natural waters. Applied Geochemistry 17, 517–568.

Stefansson, A., Seward, T.M., 2004. Gold(I) complexing in aqueous sulphide solutions to 500 °C at 500 bar. Geochimica et Cosmochimica Acta 68, 4121–4143.

Tossell, J.A., 1996. The speciation of gold in aqueous solution: a theoretical study. Geochimica et Cosmochimica Acta 60, 17–29.

Tossell, J.A., 2000. Theoretical studies on metal thioarsenites and thioantimonides, synergistic interactions between transition metals and heavy metalloids. Geochemical Transactions. doi:10.1186/1467-4866-1-16.

Voicu, G., Hallbauer, D.K., 2005. Determination of the physico-chemical characteristics of hydrothermal fluids from the post-metamorphic Omai gold deposit, Guiana Shield, using analysis of ionic species by crush-leach technique and capillary electrophoresis. Mineralogy and Petrology 83, 243–270.

Weber, L., 1997. Handbuch der Lagerstätten der Erze, Industrieminerale und Energierohstoffe Österreichs. Archiv für Lagerstättenforschung der Geologischen Bundesanstalt 19 607 pp.

Weber, L., Pausweg, F., Medwenitsch, W., 1972. Zur Mitterberger Kupfervererzung (Mühlbach/ Hochkönig) Salzburg. Mitteilungen der Österreichischen Geologischen Gesellschaft 65, 137–158.

Webster, J.G., 1986. The solubility of gold and silver in the system $Au–Ag–S–O_2–H_2O$ at 25 °C and 1 atm. Geochimica et Cosmochimica Acta 50, 1837–1845.

Webster, J.G., Mann, A.W., 1984. The influence of climate, geomorphology and primary geology on the supergene migration of gold and silver. Journal of Geochemical Exploration 22, 21–42.

Wilkin, R., Wallschlager, D., Ford, R., 2003. Speciation of arsenic in sulfidic waters. Geochemical Transactions 4, 1–7.

Xu, Y., Schoonen, M.A.A., Nordstrom, D.K., Cunningham, K.M., Ball, J.W., 1998. Sulfur geochemistry of hydrothermal waters in Yellowstone National Park: I. The origin of thiosulfate in hot spring waters. Geochimica et Cosmochimica Acta 62, 3729–3743.

Please cite this article as: Kucha, H., Raith, J.G., Gold-oxysulphides in copper deposits of the Greywacke Zone, Austria: A mineral chemical and infrared fluid inclusion study, Ore Geology Reviews (2008), doi:10.1016/j.oregeorev.2008.10.004